

NAVIGATION CONTROL OF AN X-Y PLANAR ROCKET

by

Kaung Soe Thar

A Thesis Submitted in Partial Fulfillment of the Requirements for the Degree of
Master of Engineering in Mechatronics

Examination Committee: Prof. Manukid Parnichkun (Chairperson)
Dr. Pisut Koomsap
Dr. Mongkol Ekpanyapong

Nationality: Myanmar

Previous Degree: Bachelor of Engineering in Mechatronics
Thanlyin Technological University
Myanmar

Scholarship Donor: AIT Fellowship


Asian Institute of Technology
School of Engineering and Technology
Thailand
May 2021

AUTHOR'S DECLARATION

I, Kaung Soe Thar, declare that the research work carried out for this thesis was in accordance with the regulations of the Asian Institute of Technology. The work presented in it are my own and has been generated by me as the result of my own original research, and if external sources were used, such sources have been cited. It is original and has not been submitted to any other institution to obtain another degree or qualification. This is a true copy of the thesis, including final revisions.

Date: 7th May, 2021

Name : Kaung Soe Thar

Signature: 

ACKNOWLEDGEMENTS

Firstly, I can't express my appreciation to my committee chair Professor Manukid Parnichkun and other committee members for their suggestions and their kindness all the way down to get this Master Degree.

Secondly, I express my thankfulness to my father and mother who let me to study in Asian Institute of Technology and support all the things that I would like to do in my life. Without yours kind and strong support, I can't do anything furthermore.

Thirdly, I would like to give my gratitude to my girl Khin Yadana Kyaw and my close friends Htet Wai Yan, Soe Maung Maung Oo. Thank you for your encouragements and suggestions when the time I feel depress and I need some helps.

And I would like to express my gratefulness to Mr. Prasittichai Naronglerdrit who is the Doctoral student of ISE, for helping me to use his 3D printer in the lab giving me some valuable suggestions concerning with my thesis, and other ISE lab members and friends, borrowing the things that I need, giving me suggestions and their precious time to finish my thesis. Also my teachers from Yangon Technological University and my friends from Myanmar who help me to get this degree, I really be thankful for your supports and your ideas.

And finally, I would like to thank to Asian Institute of Technology to let me study under the school compound and enjoy my second time university student life and allow me to become proud AIT alumni.

ABSTRACT

As modern technologies become so advanced, the systems have become smaller and more powerful. As aerospace engineering problems are non-linear and highly unstable, it needs a good control system to obtain better results. In this thesis, the autopilot system is implemented in small-scale rocket. To develop this system, PID controller is used to control the thrust vector (which is known as TVC), magnetometer is used to know the direction with the combination of the GPS to reach to a desired target.

CONTENTS

	Page
ACKNOWLEDGEMENTS	iii
ABSTRACT	iv
LIST OF TABLES	vii
LIST OF FIGURES	viii
CHAPTER 1 INTRODUCTION	1
1.1 Background for the Missile	1
1.2 Statement of the Problem	2
1.3 Objectives of the Research	2
1.4 Scopes and Limitations	2
CHAPTER 2 LITERATURE REVIEW	3
2.1 Missile Autopilot System	3
CHAPTER 3 METHODOLOGY	11
3.1 Overviews of the Whole System	11
3.2 System Design	11
3.2.1 Electrical Components	12
3.2.2 Dynamics of the System	20
3.2.3 Nozzle Design of the System	24
3.2.4 Finalize Electronics and Hardware Design	28
3.2.5 Tracking System Implementation	31
3.2.6 Conventional Proportional-Integral-Derivative Controller	36
3.2.7 Control Implementation	38
3.3 Water Rocket	40
3.3.1 Water Rocket Concepts	40
3.3.2 Takeoff Early State Calculation	40
3.3.3 Hardware for Water Rocket	42

CHAPTER 4 RESULTS AND DISCUSSION	44
4.1 Creating Thrust Force for Flying	44
4.2 Water Rocket Analysis	45
4.2.1 Water Rocket Simulation Analysis	45
4.3 Results of Computational Fluid Dynamics Analysis (CFD) on Nozzle 47	
4.3.1 Fluid Properties	52
4.4 Experimental Analysis Between Two Nozzle Thrust Force	53
4.5 Experimental Environment	54
4.6 Comparison Between 2 nd Order Butterworth Filter and Kalman Filter	55
4.7 GPS Point Tracking	56
CHAPTER 5 CONCLUSION AND RECOMMENDATION	62
5.1 Conclusion	62
5.2 Recommendation	62
REFERENCES	63

LIST OF TABLES

Tables		Page
Table 3.1	Arduino Due Specification	12
Table 3.2	BNO055 Data Output	13
Table 3.3	GPS Ublox 6M Specification	14
Table 3.4	Servo Motor SG90 Specification	15
Table 3.5	Micro SD Card Module Specification	16
Table 3.6	L298 Motor Driver Specification	17
Table 3.7	Solenoid Specification	17
Table 3.8	Lithium Battery Specification	18
Table 3.9	Specification of the Model	28
Table 3.10	Effects of Increasing PID Parameters	37
Table 4.1	Parameters for Water Rocket Simulation	45
Table 4.2	Modeling Geometry of Nozzle (1)	48
Table 4.3	Modeling Geometry of Nozzle (2)	50
Table 4.4	Velocity and Pressure Comparison Between Two Nozzles	51
Table 4.5	Specification of Air	52
Table 4.6	Specification of Boundary Conditions	52
Table 4.7	Root Mean Square Error for Comparison Between Two Filters	55
Table 4.8	Root Mean Square Error of Distance and Yaw for GPS 5 Points	61

LIST OF FIGURES

Figures		Page
Figure 2.1	Autopilot Design for BTT Missile	3
Figure 2.2	Aerodynamics Parameters of Class of BTT Missile for Different Operation Points (S. Mahaboob Basha & Akhilesh Swarup., 2017)	4
Figure 2.3	Disturbance Observer of Class of BTT Missile for Different Operation Points (S. Mahaboob Basha & Akhilesh Swarup., 2017)	5
Figure 2.4	Composite Control Structure of Autopilot Design (Jun Yang and Shihua Li., 2012)	6
Figure 2.5	Simulation Parameters (S. E. Talole, A.A. Godbole, J. P. Kolhe, S. B. Phadke., 2011)	7
Figure 2.6	System Block Diagram (S. E. Talole, A.A. Godbole, J. P. Kolhe, S. B. Phadke., 2011)	7
Figure 2.7	Curves for Angle of Attack and the Sideslip Angle (Ming-Zhe Hou and Guang-Ren Duan., 2011)	8
Figure 2.8	Open Loop DG Guidance and Control System (Chaoyong Li and Wuxing Jing., 2006)	9
Figure 2.9	Coordinate Frame and Geometry (Chaoyong Li and Wuxing Jing., 2006)	9
Figure 2.10	(a) Properties of Air and Gas and (b) Boundary Conditions (Varada Anil Hemanth and U.S.Jyothi , 2020)	10
Figure 2.11	Comparison for Exit Velocity, Pressure and Temperature for Air and Gas Analysis (Varada Anil Hemanth and U.S.Jyothi , 2020)	10
Figure 3.1	Simple Overview of the Missile Autopilot System	11
Figure 3.2	Arduino Due	13
Figure 3.3	BNO055	14
Figure 3.4	NEO 6M Ublox GPS Module	15
Figure 3.5	SG90 Servo Motor	16
Figure 3.6	MicroSD Card Module	16
Figure 3.7	L298 Motor Driver and Solenoid Valve	18

Figures	Page
Figure 3.8 Soaring 1000mAh 11.1V 30C 3S1P Lipo Battery	19
Figure 3.9 Electronics Connection Map	19
Figure 3.10 Rotations Between the 3D Planes	20
Figure 3.11 Forces Action Upon the Missile	21
Figure 3.12 de Laval Nozzle, with Velocity Flow Increasing from Green to Red	24
Figure 3.13 4 Types of Nozzle Expansions (1) Optimum, (2) Under Expanded, (3) Slightly Over Expanded and (4) Over Expanded	25
Figure 3.14 Typical Nozzle System	26
Figure 3.15 The Aerodynamics Calculator From dept.aoe.vt.edu/~devenpor/aoe3114/calc.html	27
Figure 3.16 Finalize Electronics Circuit (1) Top View (2) Side View and (3) Bottom View	29
Figure 3.17 Finalize Hardware Construction (1) Top View (2) Side View	29
Figure 3.18 Back Casing	30
Figure 3.19 Finalize Nozzle Designs	30
Figure 3.20 Overall Electronics Components Connection	31
Figure 3.21 Response of Butterworth LPF According to the Orders	32
Figure 3.22 Kalman Filter Algorithmic Loop	33
Figure 3.23 Haversine Formula for Waypoint Tracking	34
Figure 3.24 Path Comparison Between with Direct Point and with Intersection Points	35
Figure 3.25 Block Diagram for PID Controller	36
Figure 3.26 Overall Block Diagram of the Autopilot System	39
Figure 3.27 Flowchart of the System	39
Figure 3.28 Water Rocket Simulation From ' http://polyplex.org/rockets/simulation '	42
Figure 3.29 Water Rocket Models	42
Figure 3.30 Water Rocket Launcher	43
Figure 3.31 Water Rocket Launcher	43
Figure 4.1 Sugar Rocket Prototype	44
Figure 4.2 Water Rocket Simulation Results (a) Bottle (1) and (b) Bottle (2)	46
Figure 4.3 Bottle (1) Graph for (a) Altitude (b) Speed (c) Acceleration (d) Thrust	46

Figures	Page
Figure 4.4 Bottle (2) Graph for (a) Altitude (b) Speed (c) Acceleration (d) Thrust	47
Figure 4.5 Water Bottle Rocket Failures	48
Figure 4.6 Nozzle(1) Dimensions	49
Figure 4.7 CFD Analysis of Nozzle (1) Showing (a)Pressure Cut Plots and (b)Velocity Cut Plots	49
Figure 4.8 Nozzle(2) Dimensions	50
Figure 4.9 CFD Analysis of Nozzle (2) Showing (a)Pressure Cut Plots and (b)Velocity Cut Plots	51
Figure 4.10 Experimental Setup for Thrust Analysing	53
Figure 4.11 The Thrust Comparison Between Two Nozzle	54
Figure 4.12 The Air Outlets from Mechatronics Lab	55
Figure 4.13 Comparison Between Two Filters for Magnetometer's Heading Data	56
Figure 4.14 GPS Coordinates for Point 1	56
Figure 4.15 Yaw and Distance Error for Point 1	57
Figure 4.16 GPS Coordinates for Point 2	57
Figure 4.17 Yaw and Distance Error for Point 2	58
Figure 4.18 GPS Coordinates for Point 3	58
Figure 4.19 Yaw and Distance Error for Point 3	59
Figure 4.20 GPS Coordinates for Point 4	59
Figure 4.21 Yaw and Distance Error for Point 4	60
Figure 4.22 GPS Coordinates for Point 5	60
Figure 4.23 Yaw and Distance Error for Point 5	61

CHAPTER 1

INTRODUCTION

1.1 Background for the Missile

Rockets are developed more than 2,000 years ago. The ancient Chinese started the rockets with the gunpowder-fill cylinders. Around 1232, in the war of Chinese and Mongols, the first rocket is used.

First missile that developed by Nazi Germany during World War II was the V-2 Rocket. Hermann Oberth, a German scientist, wrote a book about rocket travel that inspired numerous rocket clubs around the world, the advent of model rocketry. One of such groups, the Verein fur Raumschiffahrt (Society for Space Travel), went on to develop numerous rockets, and during World War II the V2 (under the direction of Wernher von Braun). After the allied victory, German scientist and technology were divided between the Soviet Union and the United States, which lead to the development of intercontinental ballistic missiles, and from there the space race and exploration.

Missiles can be divided into two categories: guided missile and unguided missile. Guidance missile – fired towards a designated target and in the same time, it receives a steering control commands from the ground station or its onboard guidance control system to improve its precision. Unguided missile – follows the natural laws of motion under gravity to establish a ballistic trajectory.

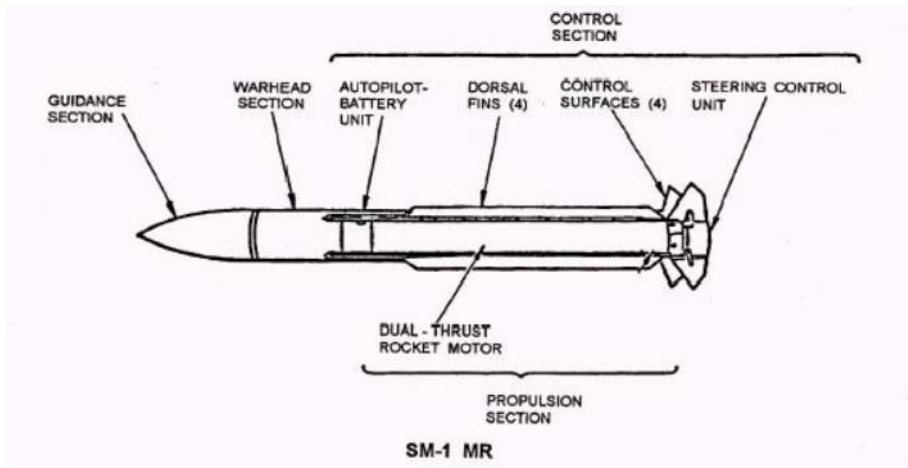
Typically, missile consists of (1) a propulsion section (sometimes called booster section), (2) control section, (3) warhead section and (4) guidance section. Mostly, missile technology has three parts, target tracking, guidance and autopilot. Target tracking – Required the accurate information concerning the position, velocity, and acceleration of the target relative to the missile. Estimators are mainly used to infer the target motion from the noisy sensor measurements, and these have their own dynamics This means that estimators will influence the tracking accuracy. Also, because of the

sensor measures distance, the estimate of velocity and acceleration will involve a form of integration with the associated errors and delays.

Figure

1.1

Typical Missile of SM-1 MR



1.2 Statement of the Problem

The robust steering of the vehicles using a variety and possibly concurrent use divert mechanisms such as aerodynamic lift, booster orientation and actuators. Use of either continuous actuators or discontinuous actuators in the presence of uncertain shock waves and actuator disturbances can cause the system unstable. This research is intended to design and develop a rocket with the compatible nozzle and a position control system to get to the desired location.

1.3 Objectives of the Research

The main objective of the research is as follow.

1. To design and develop the nozzle of the missile.
2. To develop the position control system for x-y plane of the missile.
3. To develop a trajectory tracking on x-y plane of the missile.

1.4 Scopes and Limitations

1. Small scale of the prototype which does not contain the warhead.
2. The limited booster section because of the air flow rate.
3. Only around 20m range can be achieved because of the air pressure pipe.

CHAPTER 2

LITERATURE REVIEW

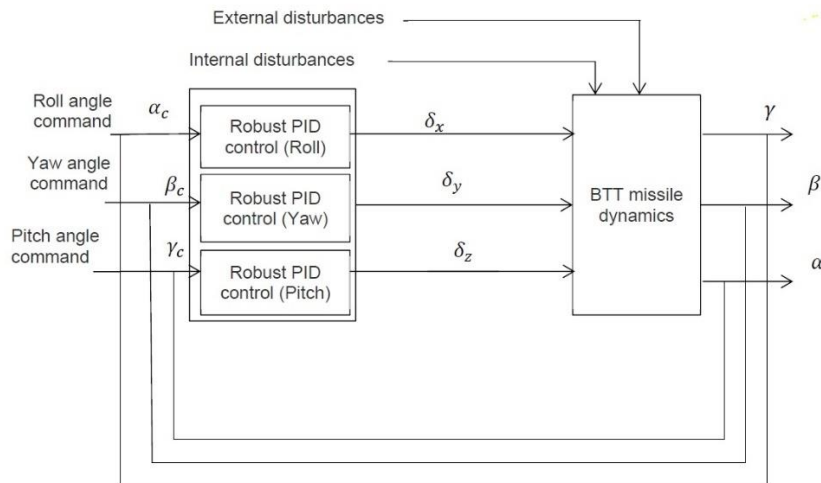
In this section, the past researchers and experiments conducted on the building the rocket and control theories on missile control. They use different methods and different control theories to get the robustness of the missile autopilot system.

2.1 Missile Autopilot System

In 2017, S. Mahaboob Basha & Akhilesh Swarup from NIT Kurukshetra (India) proposed a robust PID autopilot design for back-to-turn(BTT) missile. The concept of the robust PID autopilot is designed for the roll, pitch and yaw separately. The main contribution of this design is to stabilize each of the mentioned system and to compensate the internal and external uncertainties. The autopilot design is considered separately for each of the channel. Since it is not easy to make a controller which can control the model concerning not only non-linearity but also parameter perturbations, the non-linear parts are accounted as internal disturbances to the corresponding channels and then compensated along with external disturbances.

Figure 2.1

Autopilot Design for BTT Missile



$$\left. \begin{aligned} \dot{\omega}_z &= -(a_1 + e_1)\omega_z + (e_1a_4 - a_2)\alpha + \frac{e_1}{57.3}\omega_x\beta + (-e_1a_5 - a_3)(\delta_z + d_z) + \frac{J_x - J_y}{57.3J_z}\omega_x\omega_y \\ \dot{\alpha} &= \omega_z - \frac{1}{57.3}\omega_x\beta - a_4\alpha - a_5(\delta_z + d_z) \end{aligned} \right\}$$

Figure 2.2

Aerodynamics Parameters of Class of BTT Missile for Different Operation Points (S. Mahaboob Basha & Akhilesh Swarup., 2017)

Operating points	t ₁ (4.4 s)	t ₂ (11.7 s)	t ₃ (19.5 s)	t ₄ (23 s)	t ₅ (28 s)	t ₆ (35 s)	t ₇ (40 s)
a ₁	1.593	1.485	1.269	1.130	0.896	0.559	0.398
a ₂	260.559	266.415	196.737	137.385	129.201	66.38	51.003
a ₃	185.488	182.532	176.932	160.894	138.591	78.404	53.840
a ₄	1.506	1.295	1.169	1.130	1.061	0.599	0.421
a ₅	0.298	0.243	0.217	0.191	0.165	0.105	0.078
b ₁	1.655	1.502	1.269	1.130	1.061	0.599	0.398
b ₂	39.988	-24.627	-31.452	-41.425	-68.165	-21.448	-9.635
b ₃	159.974	170.532	182.030	184.093	154.068	89.853	59.587
b ₄	0.771	0.652	0.680	0.691	0.790	0.360	0.243
b ₅	0.254	0.191	0.188	0.182	0.162	0.102	0.072
c ₁	1.264	1.6	1.636	1.635	1.607	0.936	0.644
c ₂	1787.048	1832.067	2128.877	2231.985	3045.292	1329.481	818.706
e ₁	0.285	0.192	0.147	0.118	0.069	0.055	0.043
e ₂	0.295	0.192	0.147	0.118	0.069	0.055	0.043

The equations shown below is Kharitnov theorem, which is used for robust stability. When all equations in equation (2.2) are Hurwitz stable, the interval polynomial is robustly stable.

$$\left. \begin{aligned} K_1(s) &= a_0^- + a_1^-s + a_2^+s^2 + a_3^+s^3 + \dots \\ K_2(s) &= a_0^+ + a_1^+s + a_2^-s^2 + a_3^-s^3 + \dots \\ K_3(s) &= a_0^+ + a_1^-s + a_2^-s^2 + a_3^+s^3 + \dots \\ K_4(s) &= a_0^- + a_1^+s + a_2^+s^2 + a_3^-s^3 + \dots \end{aligned} \right\}$$

Jun Yang and Shihua Li from School of Automation, Southeast University, NanJing., 2012, the nonlinear couplings from roll, pitch, yaw channels and aerodynamics perturbations are measured as disturbances and summed up together with external disturbances by a disturbance observer (DOB) and compensated by feedforward design. The composite controller comprises High-level model predictive controller (MPC), a low-level state feedback stabilizer, and a feedforward compensator. Optimized tracking performance is done by MPC, system stabilization by low-level state feedback. The

external as well as internal disturbances formed by parameter perturbations are attenuated by feedforward compensator.

The yaw dynamics is,

$$\dot{\omega}_y = -(b_1 + e_2)\omega_y + (e_2b_4 - b_2)\beta - \frac{e_2}{57.3}\omega_x\alpha + (e_2b_5 - b_3)(\delta_y + d_y) + \frac{J_z - J_x}{57.3J_y}\omega_x\omega_z$$

$$\dot{\beta} = \omega_y + \frac{1}{57.3}\omega_x\alpha - b_4\beta - b_5(\delta_y + d_y)$$

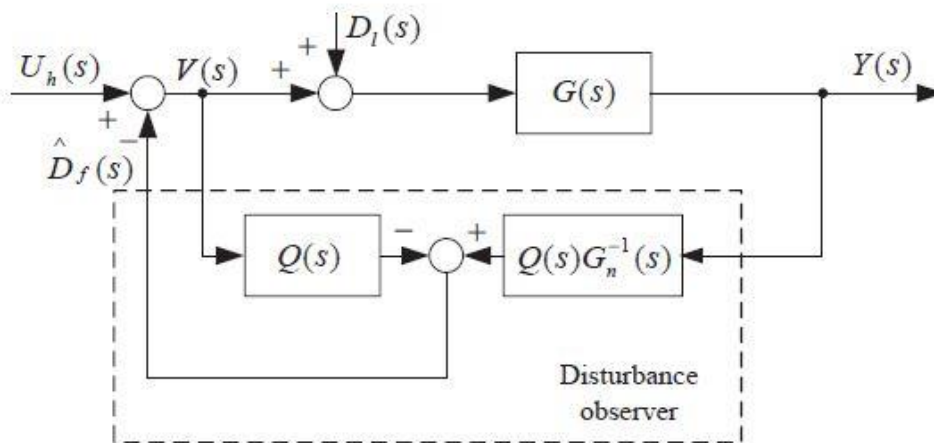
The yaw dynamics are distinguished into a linear and nonlinear parts, the state equations are formed. The composite control law for yaw channel is,

$$u = u_l + u_h + u_f$$

Where u_l is low-level control law, u_h is high-level control law and u_f is feedforward compensation control law.

Figure 2.3

Disturbance Observer of Class of BTT Missile for Different Operation Points (S. Mahaboob Basha & Akhilesh Swarup., 2017)

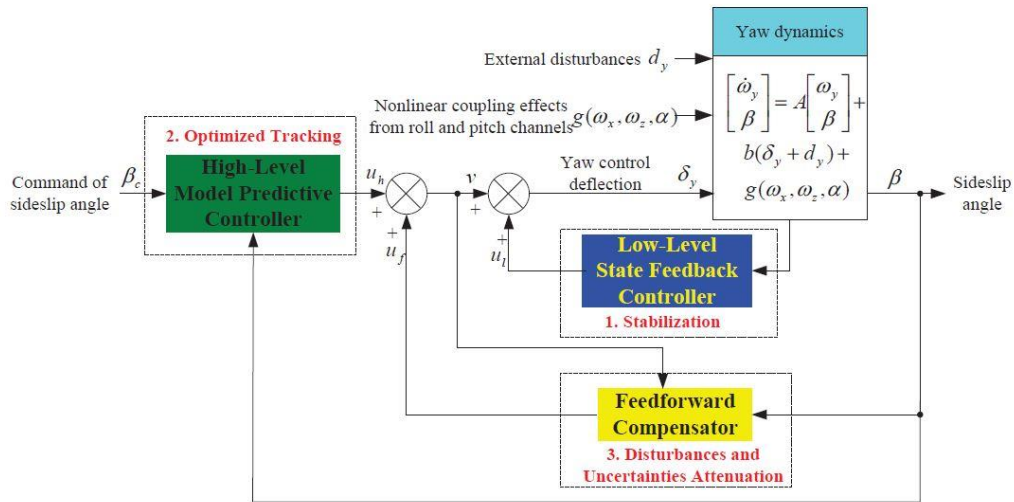


For another robust autopilot design for missile, S. E. Talole, A.A. Godbole, J. P. Kolhe from Defence Institute of Advanced Technology, India and S. B. Phadke from College of Engineering Pune, India approached three parts (1) roll autopilot for 'linear quadratic regulator (LQR)', (2) by means of the extended state observer (ESO), the effects of external disturbances and uncertainties is estimated, and (3) estimation of uncertainties and-disturbances to robust Linear Quadratic Regulator and using the state estimating to

make it implementable. Weighting factor adjustment of the Linear Quadratic Regulator is not needed as the effects of the unmodeled dynamics are reduced by the estimated states. The knowledge of uncertainties/disturbances influence are not required. The performance is compared with another 4 of the designs. Design-4 is proposed controller.

Figure 2.4

Composite Control Structure of Autopilot Design (Jun Yang and Shihua Li., 2012)



Design-1: (1) Classical Approach to achieve maximum crossover frequency for servo, rate gyro and first torsional mode.
 (2) CF (crossover frequency) is chosen high enough to obtain a wide autopilot bandwidth but not enough to avoid stability problems.
 (3) To remove the torsional effect on limitation CF, notch filter is used.
 (4) The final controller with the roll rate is Proportional Integral (PI) controller.

Design-2: (1) Design-1 also included a joint design of optimal/classical for a roll autopilot and is used for optimal design technique adding some extra constraints.
 (2) For optimal design, second-order rigid body roll dynamics is considered for LQR controller design.
 (3) The remaining concepts are the same as design-1.

- Design-3: (1) LQR controller is designed by using rigid body, second-order roll dynamics.
 (2) By adjusting the weight of the control input, the gain crossover frequency can be controlled.
- Design-4: (1) Design-1 represents a roll control with PI controller and in design-5, it is replaced with PD controller.
 (2) To get the roll angle error occurred by a disturbance moment to zero, the addition of an integral action is expected.

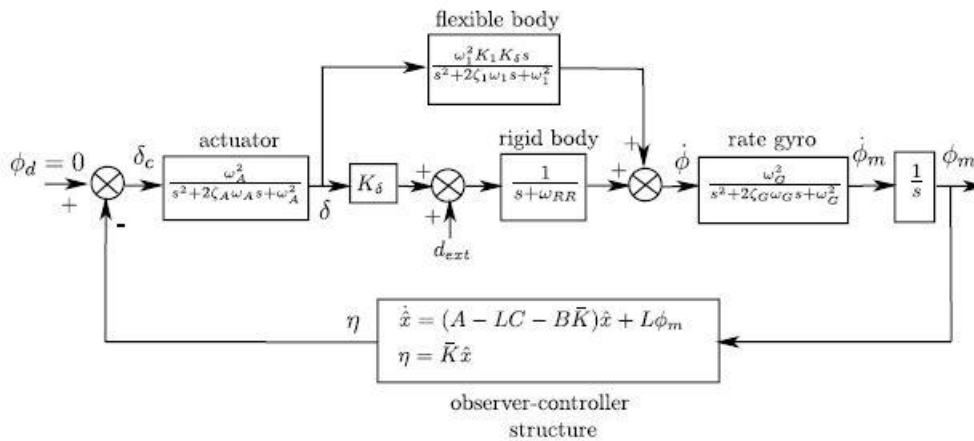
Figure 2.5

Simulation Parameters (S. E. Talole, A.A. Godbole, J. P. Kolhe, S. B. Phadke., 2011)

Design	Gains		ω_{2c} (rad/s)	Gain margin, dB	Phase margin, deg
Design-1	$F_1 = 0.0033$	$F_2 = 0.0367$	32.5	5.30	32.6
Design-2	$F_1 = 0.0037$	$F_2 = 0.0530$	36.9	3.92	23.5
Design-3	$F_1 = 0.0500$	$F_2 = 0.0035$	35.5	5.76	33.1
Design-4	-	-	33.8	3.95	18.0
Design-5	$F_1 = 0.0033$ $F_3 = 0.1500$	$F_2 = 0.0367$	31.3	5.38	32.9

Figure 2.6

System Block Diagram (S. E. Talole, A.A. Godbole, J. P. Kolhe, S. B. Phadke., 2011)

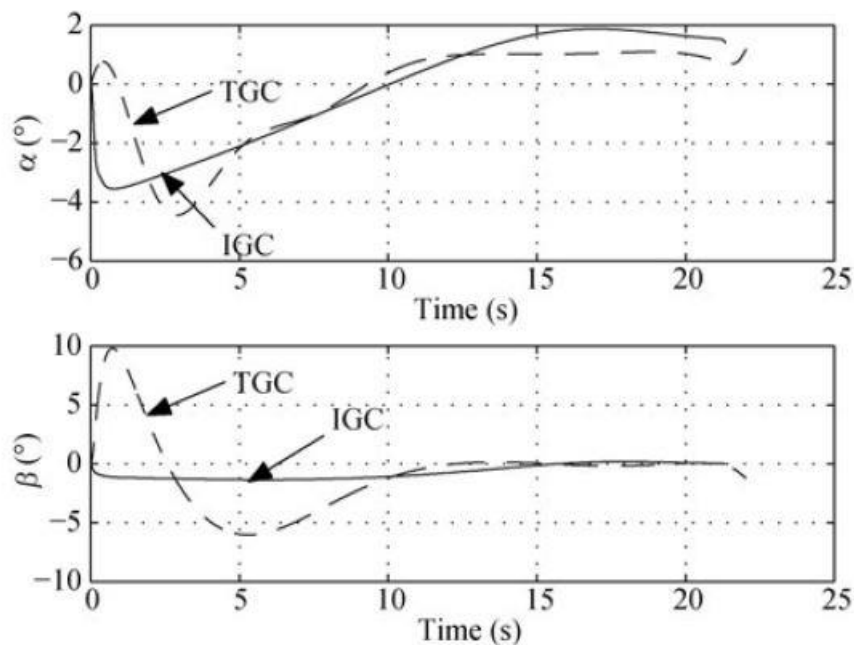


Ming-Zhe Hou and Guang-Ren Duan from Harbin Institute of Technology, PRC proposed an adaptive dynamic surface control algorithm which is provided that proposed feedback controller can guarantee both the accuracy of target interception

and the stability of the missile dynamics. The proposed method is implemented on the pitch plane but the same control method can be provided to the yaw and roll channels either. Based on the mathematical analysis for the control system, consider the integrated control and guidance control system satisfying the assumption equation. Any bounded initial states, the robust adaptive dynamic surface control algorithm can keep all the states of the closed-loop system bounded and continuously make the value of the output arbitrarily small if proper parameter values are huge enough. This is called integrated guidance and control design for pitch channel.

Figure 2.7

Curves for Angle of Attack and the Sideslip Angle (Ming-Zhe Hou and Guang-Ren Duan., 2011)



By observing the simulation results from the figure 2.7, the proposed IGC method is much better than the traditional guidance and control (TGC) which is proportional navigation guidance plus PID control law. By observing this IGC method, it can have several advantages. (1) The smaller the desired overload, the smaller the angle of attack and sideslip. (2) The flight time is shorter and (3) The error distance is much smaller. (The missile accuracy can be improved).

Chaoyong Li and Wuxing Jing from the Department of Aerospace Engineering, Harbin Institute of Technology, China., 2006, proposed the Proportional-integral-derivative (PID) controller for two-dimensional (2D) differential geometric (DG) guidance and control problem. The PID parameter are tuned by the Ziegler-Nichols (ZN) method and Routh-Hurwitz stability algorithm for a fast merging of the error.

Figure 2.8

Open Loop DG Guidance and Control System (Chaoyong Li and Wuxing Jing., 2006)

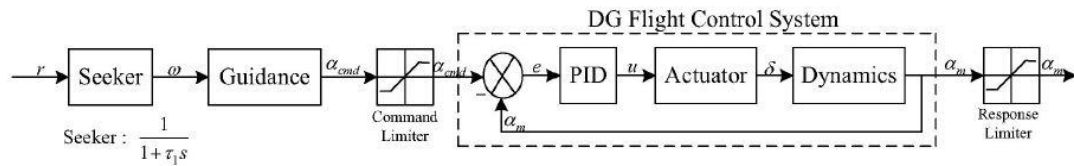
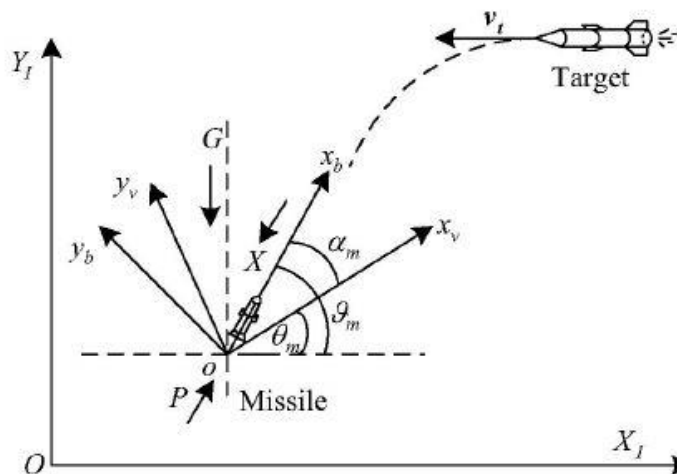


Figure 2.9

Coordinate Frame and Geometry (Chaoyong Li and Wuxing Jing., 2006)



Varada Anil Hemanth and U.S.Jyothi from mechanical department, GRIET, Hyderabad make analysis on exit parameters for nozzle pressure, temperature and velocity with a theoretical values. The analysis is carried out for both Air and Gas as operating fluids and matched with the theoretical data. The table 2.1 shows the properties of Air and Gas that authors are used in this analysis. The dimensions for the analysis are as follow: Inlet diameter is 35mm, throat diameter = 11mm, exit diameter = 17mm, radius of convergent section = 9mm, divergence angle = 13.5deg, and nozzle length = 25mm.

Figure 2.10

(a) Properties of Air and Gas and (b) Boundary Conditions (Varada Anil Hemanth and U.S.Jyothi , 2020)

Property	Air	Gas
Density(ρ)	Ideal Gas	Ideal Gas
Specific heat (C_p)	1005 J/kg.K	1820 J/kg.K
Thermal conductivity(k)	24.35 W/m.K	0.183 W/m.K
Molecular viscosity (μ)	1.716e-05 N.s/m ²	6.45e-05 N.s/m ²
Ratio of specific heats(γ)	1.4	1.2

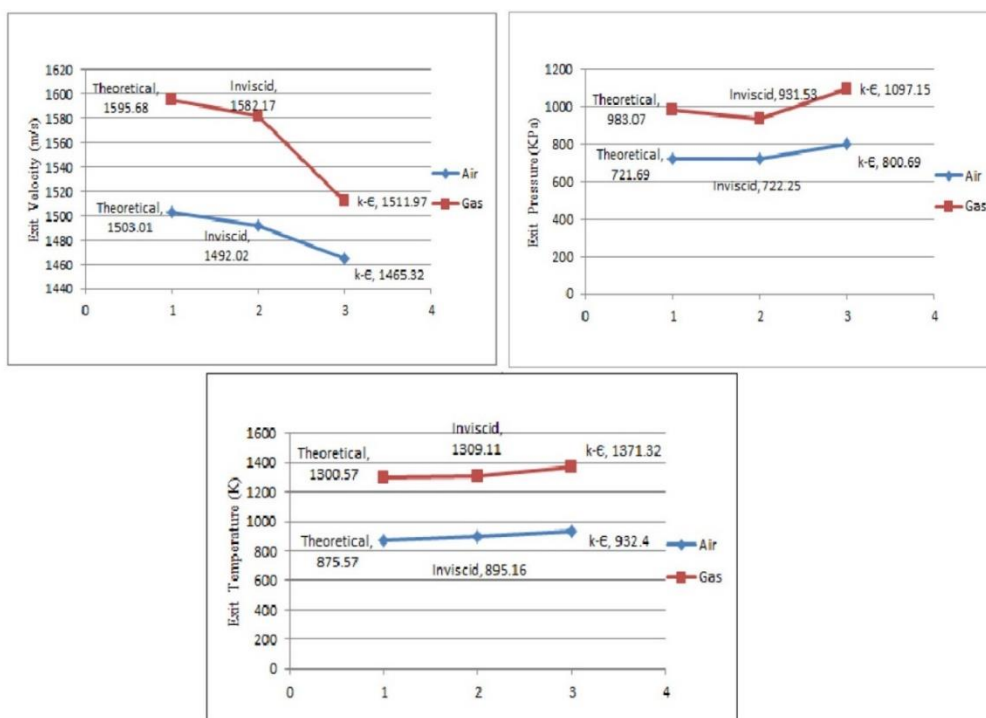
(a)

Inlet(Pressure-Inlet) Total Gauge Pressure	130bar
Initial Gauge Pressure	129.66bar
Inlet Temperature	2000k
Pressure of Operating conditions	0bar
Outlet Pressure, temperature	0bar, 300k

(b)

Figure 2.11

Comparison for Exit Velocity, Pressure and Temperature for Air and Gas Analysis (Varada Anil Hemanth and U.S.Jyothi , 2020)



CHAPTER 3

METHODOLOGY

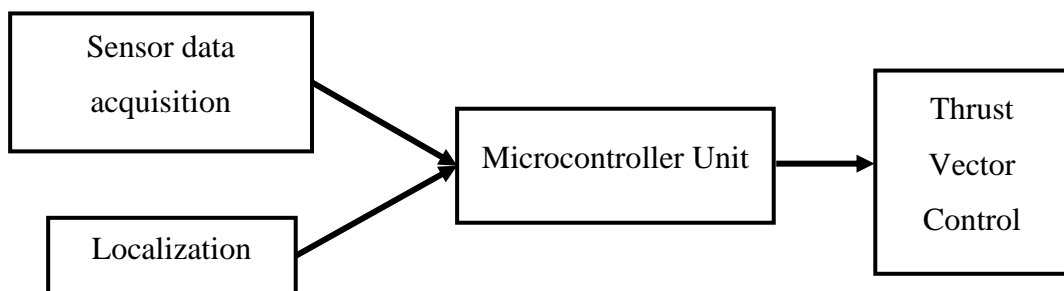
In this section, it includes three parts (1) Overviews of the whole system, (2) system design and (3) control design and software development are discussed.

3.1 Overviews of the Whole System

The system contains the small-scaled rocket body tube, the BNO sensor, which can give both gyro data and magnetometer data and GPS for localization of the position of the rocket. The actual latitude and longitude position of the rocket is taken from the GPS module and then it is calculated through the Haver-sine formula to acquire the distance and bearing angles. Then the trust vector control is used to control the yaw angle of the rocket and the solenoid valve is used to control to reach to the target position.

Figure 3.1

Simple Overview of the Missile Autopilot System



3.2 System Design

In this section, which electronics components are used in this system and the overall design of the rocket are explained.

3.2.1 Electrical Components

The following electronic components are used in this system to obtain the data, localization and driven.

1. Microcontroller
2. IMU
3. GPS
4. Servo motor
5. SD card module
6. Solenoid Valve
7. Motor Driver L298
8. Battery

The most vital and brain of the system is the microcontroller unit. It performs all the essential calculation and give control signals to the output devices what to do, how to do and when to do. Another important thing is it needs to be able to communicate with the sensors and other modules very fast. And in this system, there are a lot of communication peripherals and the microcontroller need to be very fast as well as it needs a lot of pins to connect to these devices. So, to get the fast and enough pins to connect all the modules, the Arduino Due microcontroller was chosen to cover all these requirements.

Table 3.1

Arduino Due Specification

Attribute	Specification
CPU	32-bit ARM (AT91SAM3X8E)
Clock speed	84 MHz
Operating voltage	3.3V
Flash memory & SRAM	512KB/96KB
Length x width	101.52 x 53.3
Weight	36 g
Digital IO pins & PWM pins	54/(12)

Figure 3.2

Arduino Due



Another important electronic component for this system is inertial measurement unit (IMU). There are other IMUs like MPU6050 and MPU9250 but they do not contain magnetometer. To make the electronic components compact as much as possible and to obtain roll, pitch, and yaw data as well as getting magnetometer data, the BNO055 was chosen to solve this puzzle.

Table 3.2

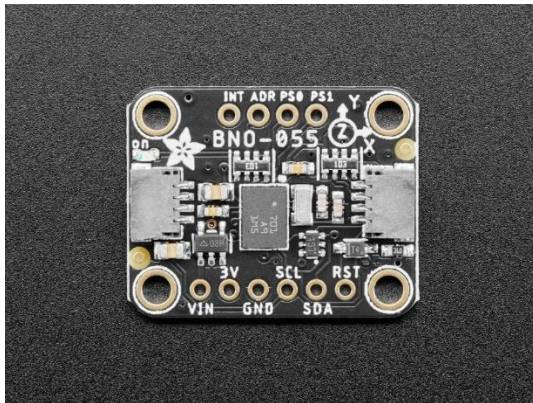
BNO055 Data Output

Sensor Data	Hz/Units
Orientation (For Euler & quaternions)	100/ (360deg and 4 point quaternions)
Vector (Angular Velocity)	100/ (rad/s)
Vector (Acceleration)	100/ (m/s ²)
Vector (Magnetic field strength)	20/ micro Tesla (uT)
Sensor Data	Hz/Units
Vector (Linear acceleration)	100/ (m/s ²)
Vector (Gravity)	100/ (m/s ²)

On the other hand, BNO055 has built in ARM Cortex-M0 based processor so the algorithms relating with sensor fusion technology are used to combine magnetometer, accelerometer, and gyroscope data into stable 3D orientation data. And it can also split data that can used in quaternions, Euler angles, or vectors. Also, BNO055 used 3.3V as an operating voltage so it is compactable with arduino due.

Figure 3.3

BNO055



GPS is used to locate the system's location (latitude and longitude). For getting GPS data, the NEO-6M Ublox module was chosen because compare to other GPS, it can give more accurate in accuracy and compactable with arduino due and it is reasonable with the price and performance. The build-in rechargeable battery acts as backup power source to provide for warm-up start even after the core power source is off. This small battery can keep the GPS receiver to store data for half an hour.

Table 3.3

GPS Ublox 6M Specification

Attribute	Specification
Cold start/ Warm start/ Hot Start	27s/ (27s)/ (1s)
Accuracy (Horizontal)	2.5m
Accuracy (Velocity)	0.1 m/s
Accuracy (Heading)	0.5 deg

Figure 3.4

NEO 6M Ublox GPS Module



To control the direction of the rocket nozzle, the “SG90” servo motor is used. It is tiny and light weighted with strong output power. It can turn around 180 deg and since the design need to be small and compact, it is the right choice to use SG90.

Table 3.4

Servo Motor SG90 Specification

Attribute	Specification
Speed	0.1s
Torque	2.5 kg-cm
Weight	15g
Operating voltage	4.8 ~ 6V

Since it is moving vehicle and the data (such as errors, time, etc) are needed to be send back to personal computer (PC), the datalogger is used. There are so many ways to send data back to PC using wireless technologies such as Xbee wireless, ESP32, Bluetooth but due to the hard setup and the working range of these devices, the micro SD card module is used as a data logger to obtain the require data from the system. The microSD card module read and connect to arduino due through SPI interface to send and obtain from the microSD card.

Figure 3.5

SG90 Servo Motor

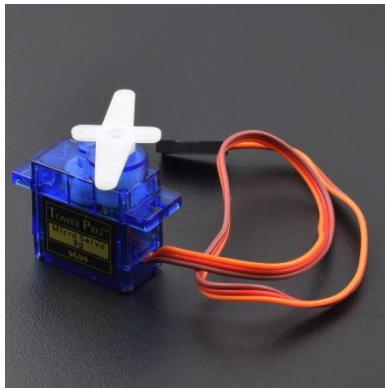


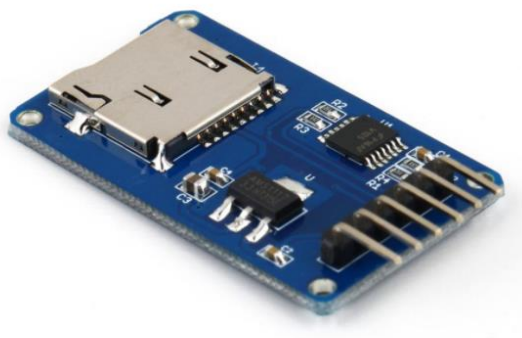
Table 3.5

Micro SD Card Module Specification

Attribute	Specification
Communication type	Serial peripheral interface (SPI)
Operating voltage	3.3 ~ 5V

Figure 3.6

MicroSD Card Module



For the propulsion system, the pressurized air is used. To determine when to stop the air flow or resume air, the 12V solenoid valve is used. Together, the L298 motor driver is used as the driver to drive the solenoid valve. Because the ampere rating of arduino

due output pins is at most 500mA and it cannot give enough current rating to give power to the solenoid valve.

Table 3.6

L298 Motor Driver Specification

Attribute	Specification
Logical voltage	5V
Drive Voltage	5~35V
Logical current	0~36mA
Drive current	2A
Max Power	25W

Table 3.7

Solenoid Specification

Attribute	Specification
Operating voltage	12V DC
Valve type	2 Ways normally closed
Operating pressure	0 ~ 1Mpa
Operating current	550mA
Max Power	6.5W

For getting enough amp rating and voltage, using relay or motor driver is the best solution for that issue. Using relay to drive the solenoid valve is heavy and it is not as fast as motor driver. The L298's logical voltage and logical is 5V and 36mA, respectively. Also, the output logic bits of the L298 are 0 to 255. The solenoid valve can be driven with digital system logic "0" or "1". It cannot drive with the pulse width modulation, so, by giving the PWM bits of the motor driver output bits to "255", it is typically work as giving "1" in digital system.

Figure 3.7

L298 Motor Driver and Solenoid Valve



Powering up the above electronic components, the size of the battery is one of the consideration factors for this system. For compacting and getting powerful battery purpose, the Lipo battery is chosen. Since the capacity and discharge rate is important in choosing the Lipo battery, the 11.1V 3S rate battery is suitable with the system.

Table 3.8

Lithium Battery Specification

Attribute	Specification
Capacity	1000mAh
Voltage/Cell	11.1V/3S
Discharge rate	30C
Weight	89g
Max Power	6.5W

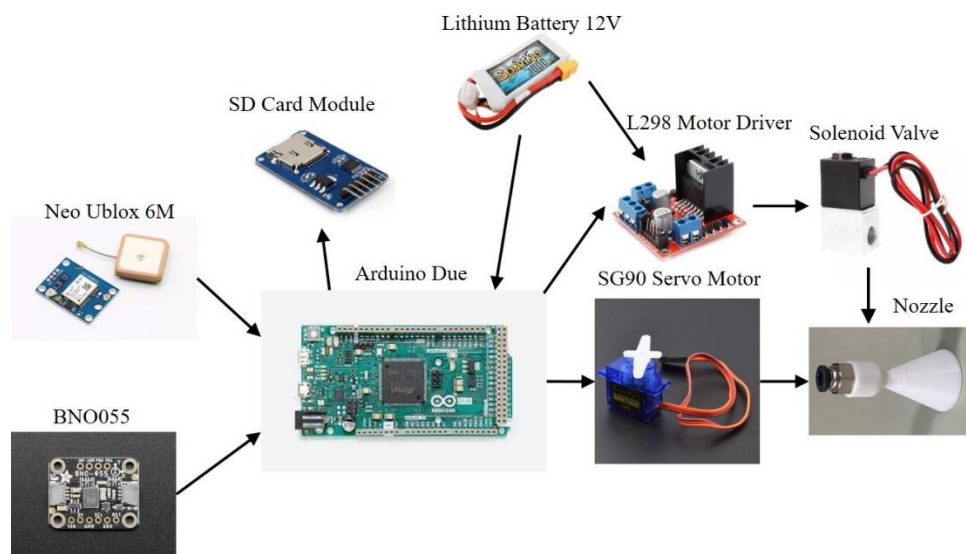
Figure 3.8

Soaring 1000mAh 11.1V 30C 3S1P Lipo Battery



Figure 3.9

Electronics Connection Map



3.2.2 Dynamics of the System

Figure 3.10

Rotations Between the 3D Planes

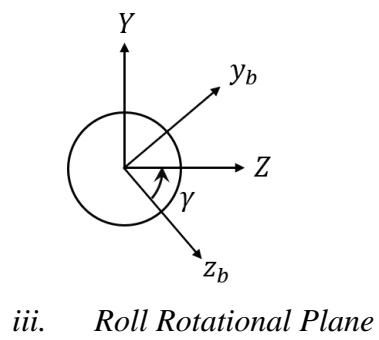
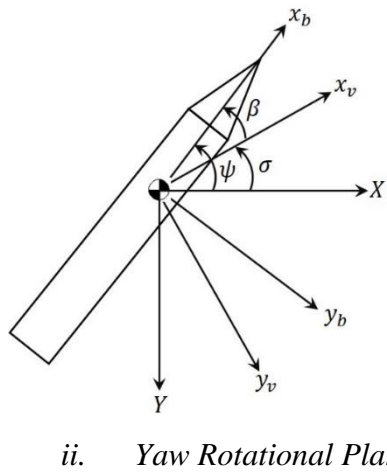
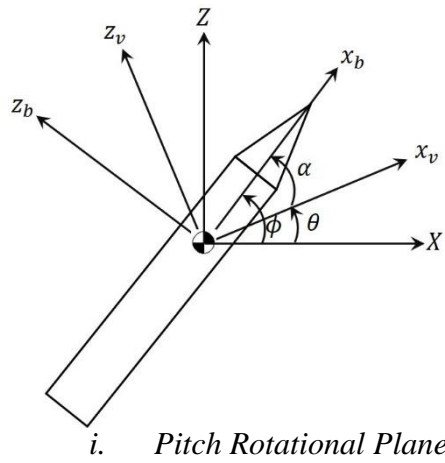
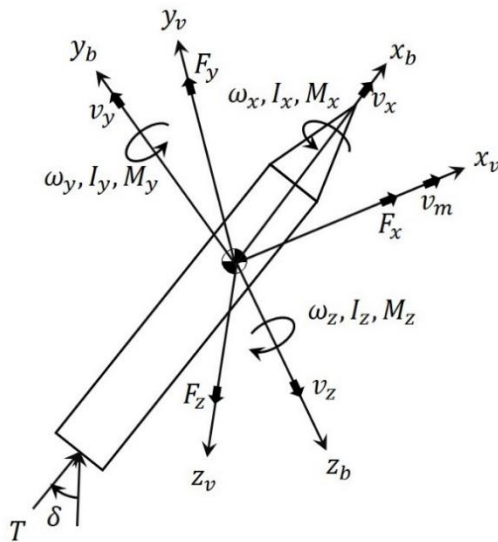


Figure 3.11

Forces Action Upon the Missile



Nomenclature for figure 3.10 and 3.11 are as follow:

F_x, F_y, F_z = Forces acting on the missile

I_x, I_y, I_z = Moment of the inertia kgm^2 / s

M_x, M_y, M_z = Total moments on the missile (Nm)

T = Thrust force (N)

v_m = velocity of the missile

X, Y, Z = reference coordinate of the missile

x_b, y_b, z_b = Body coordinate of the missile

x_v, y_v, z_v = velocity coordinate of the missile

$\omega_x, \omega_y, \omega_z$ = Angular velocity of the missile (rad/s)

γ, ϕ, ψ = Euler's angle (Roll, Pitch, Yaw)

α = Angle of attack

β = slip angle

δ_α = thrust angle for the pitch plane

δ_β = thrust angle for the yaw plane

C_x, C_{x0}, C_y, C_z = force coefficient for aerodynamics

$m_{x0}, m_{y\beta}, m_{y0}, m_{z\alpha}, m_{z0}$ = moment coefficient for aerodynamics

D = cross sectional diameter of the body

S = reference area

Q = dynamic pressure of fluid

X_{cg} = distance between center of gravity and nozzle

g = gravity constant (9.81)

Let R_1, R_2, R_3 be the rotations about X, Y and Z planes. The Euler rotation angles are normally based on the direct cosine matrix.

$$R_1 = \begin{bmatrix} 1 & 0 & 0 \\ 0 & \cos \gamma & \sin \gamma \\ 0 & -\sin \gamma & \cos \gamma \end{bmatrix}, R_2 = \begin{bmatrix} \cos \phi & 0 & -\sin \phi \\ 0 & 1 & 0 \\ \sin \phi & 0 & \cos \phi \end{bmatrix}, R_3 = \begin{bmatrix} \cos \psi & \sin \psi & 0 \\ -\sin \psi & \cos \psi & 0 \\ 0 & 0 & 1 \end{bmatrix}$$

Thus, the transformation matrix of the body can be described as:

$$\begin{bmatrix} x \\ y \\ z \end{bmatrix}_b = R \begin{bmatrix} X \\ Y \\ Z \end{bmatrix}, \text{ Where } R = R_1 R_2 R_3 \text{ which can be called 321-rotation sequence}$$

For the reference coordinates according to the body reference system is:

$$\begin{bmatrix} X \\ Y \\ Z \end{bmatrix} = R^T \begin{bmatrix} x \\ y \\ z \end{bmatrix}_b, \text{ where } R^T \text{ is the inverse matrix of } R$$

By using Euler's angle can happen the gimbal lock, which is the failure of 1DOF in 3D plane. To avoid that gimbal lock effect, the quaternions is used. Quaternions is three axes, four-parameter system of real numbers, which can be defined as a three-dimensional vector in form:

$$q = q_0 + q_1 i + q_2 j + q_3 k$$

Where q_0, q_1, q_2, q_3 represents real numbers and i, j and k are basic of quaternion vectors. For orthogonally, it can be represented as:

$$q_0^2 + q_1^2 + q_2^2 + q_3^2 = 1$$

Normally, the IMU can only provide the Euler angles. To get the quaternions, the equations between quaternions and Euler angles are used. The relation between quaternions and Euler angles are as follow:

$$q_0 = \cos(\psi / 2) \cos(\gamma / 2) \cos(\phi / 2) - \sin(\psi / 2) \sin(\gamma / 2) \sin(\phi / 2)$$

$$q_1 = \cos(\psi / 2) \sin(\phi / 2) \sin(\gamma / 2) + \sin(\psi / 2) \cos(\phi / 2) \cos(\gamma / 2)$$

$$q_2 = \cos(\psi / 2) \sin(\phi / 2) \cos(\gamma / 2) - \sin(\psi / 2) \cos(\phi / 2) \sin(\gamma / 2)$$

$$q_3 = \cos(\psi / 2) \cos(\phi / 2) \sin(\gamma / 2) + \sin(\psi / 2) \sin(\phi / 2) \cos(\gamma / 2)$$

The translation of the matrix regarding to the quaternion can be expressed as:

$$R_q = \begin{bmatrix} q_0^2 + q_1^2 - q_2^2 - q_3^2 & 2(q_1q_2 - q_0q_3) & 2(q_1q_3 + q_0q_2) \\ 2(q_1q_2 + q_0q_3) & q_0^2 - q_1^2 + q_2^2 - q_3^2 & 2(q_2q_3 - q_0q_1) \\ 2(q_1q_3 - q_0q_2) & 2(q_2q_3 + q_0q_1) & q_0^2 + q_1^2 - q_2^2 + q_3^2 \end{bmatrix}$$

For the dynamical model of a missile as show in figure 3.9,

$$F_x = m\dot{V}_m$$

$$F_y = mV_m\dot{\theta}$$

$$F_z = -mV_m \cos(\theta)\dot{\sigma}$$

$$M_x = I_x\dot{\omega}_x - (I_y - I_z)\omega_y\omega_z$$

$$M_y = I_y\dot{\omega}_y - (I_z - I_x)\omega_z\omega_x$$

$$M_z = I_z\dot{\omega}_z - (I_x - I_y)\omega_x\omega_y$$

$$\dot{X} = V_m \cos(\theta) \cos(\sigma)$$

$$\dot{Y} = V_m \sin(\theta)$$

$$\dot{Z} = -V_m \cos(\theta) \sin(\sigma)$$

$$\dot{\psi} = (\omega_y \cos(\gamma) - \omega_z \sin(\gamma)) / \cos(\phi)$$

$$\dot{\phi} = \omega_y \sin(\gamma) + \omega_z \cos(\gamma)$$

$$\dot{\gamma} = \omega_x - \dot{\psi} \sin(\phi)$$

The forces and moments behaving on the system are caused by aerodynamics of the rocket, thrust force and gravity.

$$F_x = T \cos(\alpha - \delta_\alpha) \cos(\beta - \delta_\beta) - QS(C_{x0} + C_x(\alpha^2 + \beta^2)) - mg \sin(\theta)$$

$$F_y = T \sin(\alpha - \delta_\alpha) + QSC_y\alpha - mg \cos(\theta)$$

$$F_z = -T \cos(\alpha - \delta_\alpha) \sin(\beta - \delta_\beta) - QSC_z \beta$$

$$M_x = DQS m_{x0} \frac{\omega_x D}{2V_m}$$

$$M_y = -T \cos(\delta_x) \sin(\delta_\beta) X_{cg} + DQS \left(m_{y\beta} \beta + m_{y0} \frac{\omega_y D}{V_m} \right)$$

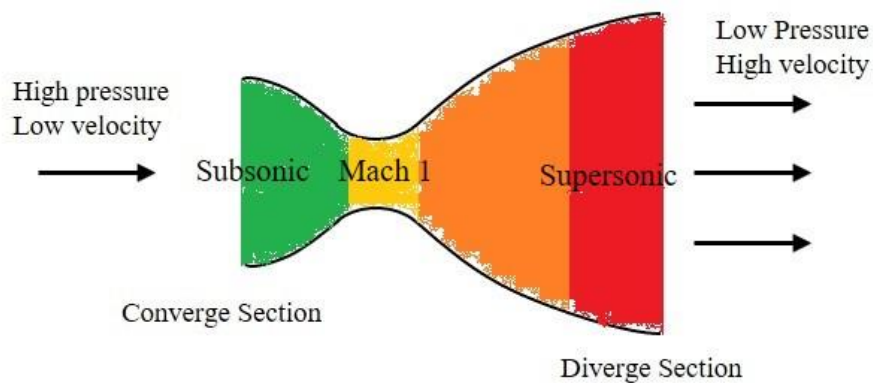
$$M_z = T \sin(\delta_\alpha) X_{cg} + DQS \left(m_{z\alpha} \beta + m_{z0} \frac{\omega_z D}{V_m} \right)$$

3.2.3 Nozzle Design of the System

The nozzle is the important factor for the rocket design process. To obtain the maximum thrust force from the combustion of the fuels, the nozzle plays in the important roles. The main function of the nozzle is to accelerate the gases that is produced by combusting the fuels. By means of that, it produces the high velocities at the exit of the nozzle. Mostly, the nozzles are based on converging-diverging nozzle or CD nozzle (also known as de Laval nozzle). There are three types of nozzle, (1) Cone which is conical and linear, (2) Bell-shaped nozzle which is classic converging-diverging nozzle, and Annular which is expansion-deflection type. Among them, in this thesis, the conical nozzle is used.

Figure 3.12

de Laval Nozzle, with Velocity Flow Increasing from Green to Red



The optimal expansion of the nozzle is the best for the nozzle which can works effectively in the desired conditions. If the nozzle is over or under expanded, the efficiency loss will be happened in that ideal nozzle.

Figure 3.13

4 Types of Nozzle Expansions (1) Optimum, (2) Under Expanded, (3) Slightly Over Expanded and (4) Over Expanded

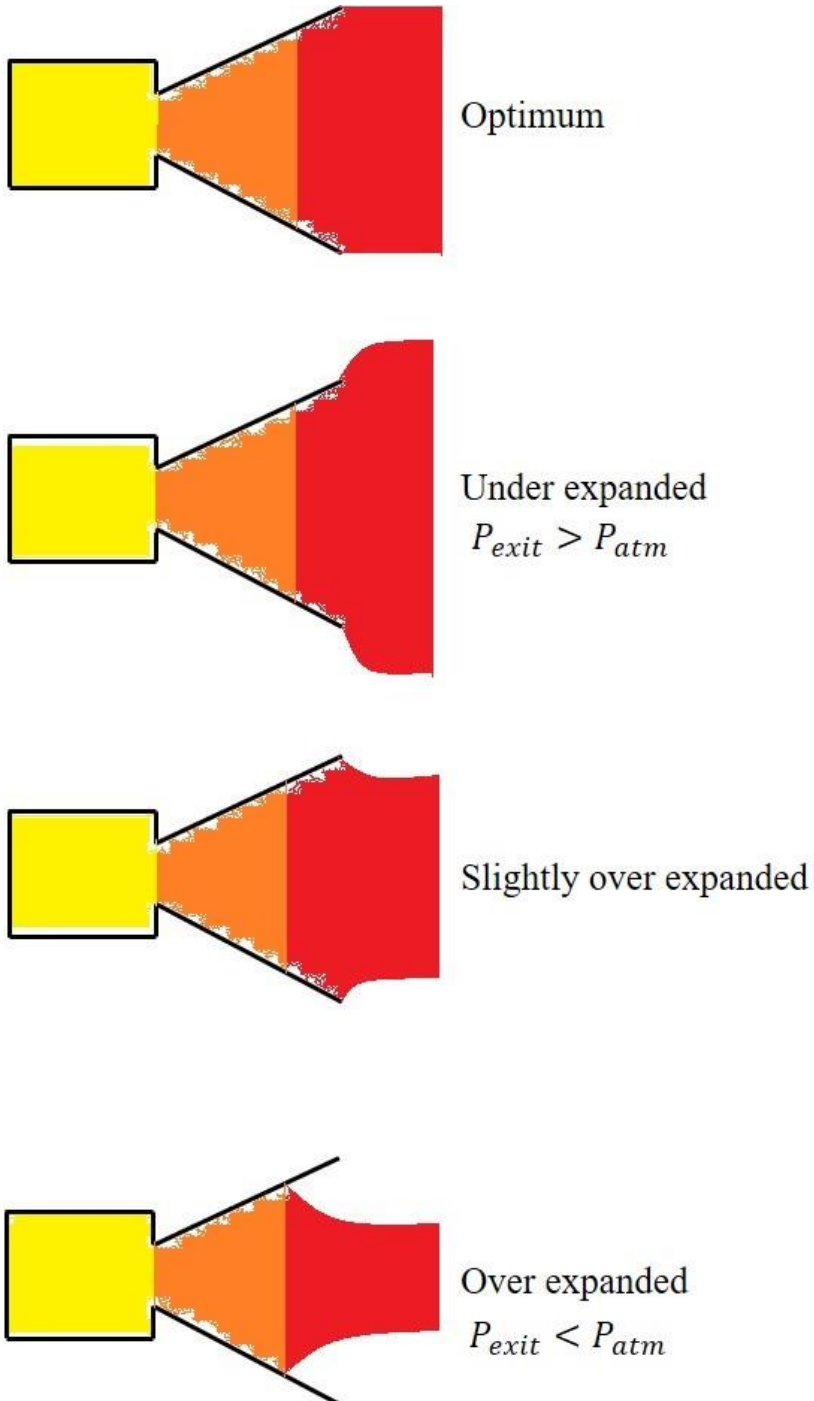
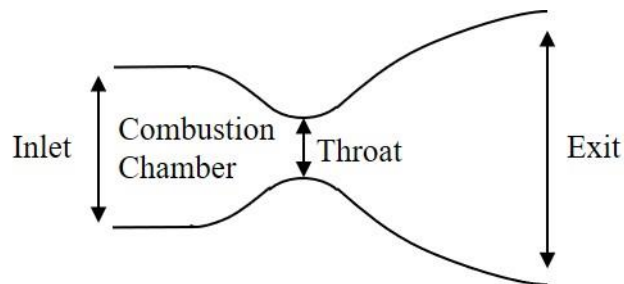


Figure 3.14

Typical Nozzle System



As nozzle throat diameter and exit diameter are important to get a good nozzle, the step by step following general equations for the design of the nozzle are used to find the throat and exit diameter.

$$\omega_t = F / I_{sp}$$

ω_t = total propellant flow rate, F = the required thrust force, I_{sp} = impulse rate

$$A_t = \frac{\omega_t}{P_t} \sqrt{\frac{RT_t}{\gamma g}}$$

Where R = gas constant, g = 9.81 and γ = the heat capacity ratio for the gas, A_t = throat's area, T_t = throat temperature

At choke condition, at the throat of the nozzle, the Mach number be "1".

To get the temperature ratio of the throat T_t and the chamber T_c ,

$$T_t = T_c \left[\frac{1}{1 + \frac{\gamma - 1}{2}} \right]$$

To get the pressure ratio of the throat pressure P_t and the chamber temperature P_c ,

$$P_t = P_c \left[1 + \frac{\gamma - 1}{2} \right]^{-\frac{\gamma}{\gamma - 1}}$$

For getting Mach number of the nozzle, the following equation can be used.

$$M_e^2 = \frac{2}{\gamma - 1} \left[\left(\frac{P_c}{P_{atm}} \right)^{\frac{\gamma - 1}{\gamma}} - 1 \right]$$

Or according to the design's requirement, the following website can be used as the alternative way to find the Mach number of the nozzle.

Figure 3.15

The Aerodynamics Calculator From dept.aoe.vt.edu/~devenpor/aoe3114/calc.html

By changing the heat capacity ratio (and changing the input, the Mach number, as well as the pressure ratio, the temperature ratio and the area ratio of the nozzles can be obtained. It is used according to the system's requirements. Some of the conditions, the one can get the ratio of the areas, or the pressure or the temperature. In that situations, the Mach number can be found easily.

By continuing the design equations, the exit area of the nozzle is:

$$A_e = \frac{A_t}{M_e} \left[\frac{1 + \frac{\gamma - 1}{2} M_e^2}{\frac{\gamma + 1}{2}} \right]^{\frac{\gamma + 1}{2(\gamma - 1)}}$$

$$D_t = \sqrt{\frac{4A_t}{\pi}}$$

$$D_e = \sqrt{\frac{4A_e}{\pi}}$$

The length of the combustion chamber can be found by using following equation.

$$A_c = \frac{\pi D_c^2}{4}$$

$$V_c = 1.1 \left(\frac{A_c}{L_c} \right)$$

$$L^* = \frac{V_c}{A_t}$$

L^* is the characteristic length of the combustion chamber. The characteristic chamber length is defined as the length of a chamber of the same size with a straight tube and no converging nozzle section.

The ideal thrust force equation and exit velocity can be described as follow:

$$Thrust = F_t = \dot{m}V_e + (P_e - P_0)A_e$$

$$V_e = M_e \sqrt{R\gamma T_e}$$

3.2.4 Finalize Electronics and Hardware Design

Table 3.9

Specification of the Model

Attribute	Specification
Tube length	610mm
Tube diameter	101.6mm
Total weight	1.2kg
Wheel diameter	72mm
Air pipe diameter (ID x OD)	4x6mm
Air pipe	Polyurethane

The body tube type is the phenolic tube, which is impregnated with the resin, treated with heat and very strong in strength. At the end of the tube, there is the end capped casing which is intended to hold the servo motor with the nozzle. The electronics components are inserted inside the tube. The GPS is attached to the body tube because the GPS needs to get the satellite data, so it needs to be in open space. To provide the air pressure, the polyurethane tube is used. It is versatile, flexible, high pressure withstand able, and strong in surface.

Figure 3.16

Finalize Electronics Circuit (1) Top View (2) Side View and (3) Bottom View

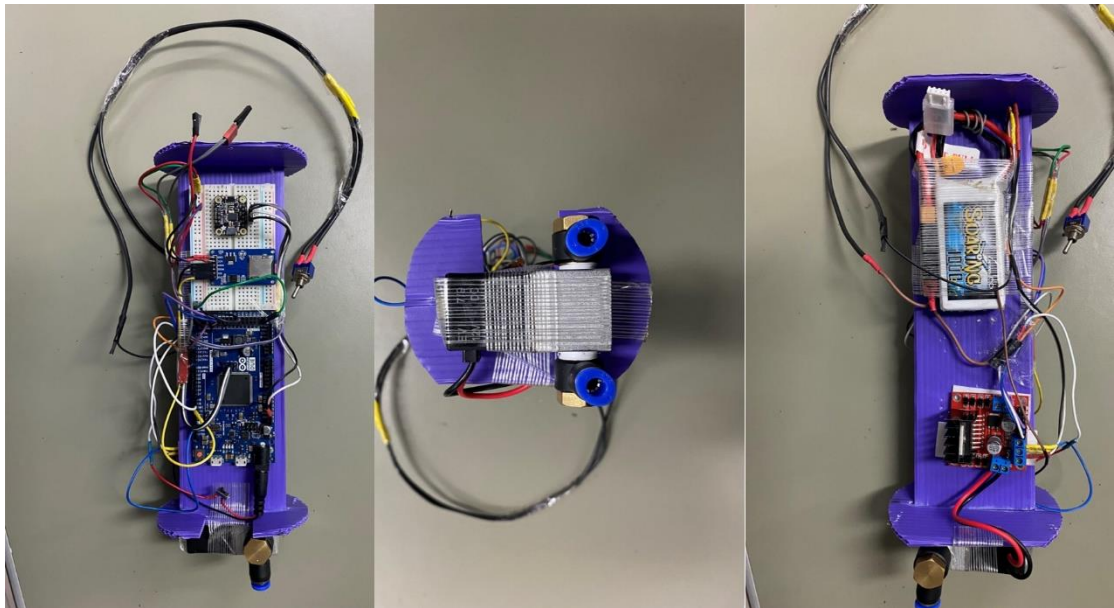
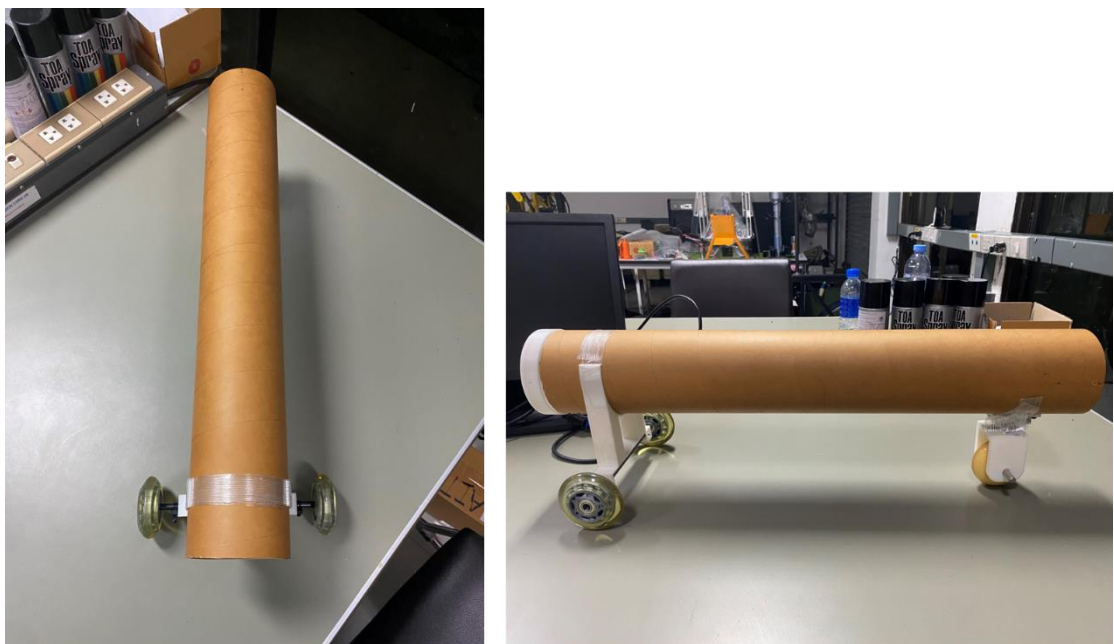


Figure 3.17

Finalize Hardware Construction (1) Top View (2) Side View



Top view

Side View

Figure 3.18

Back Casing

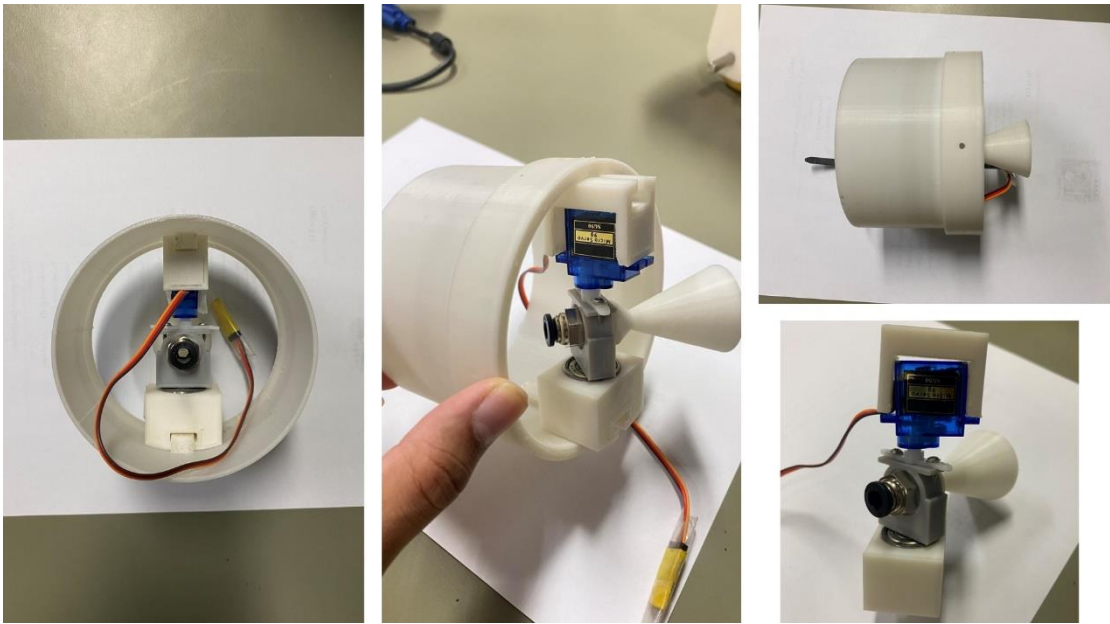


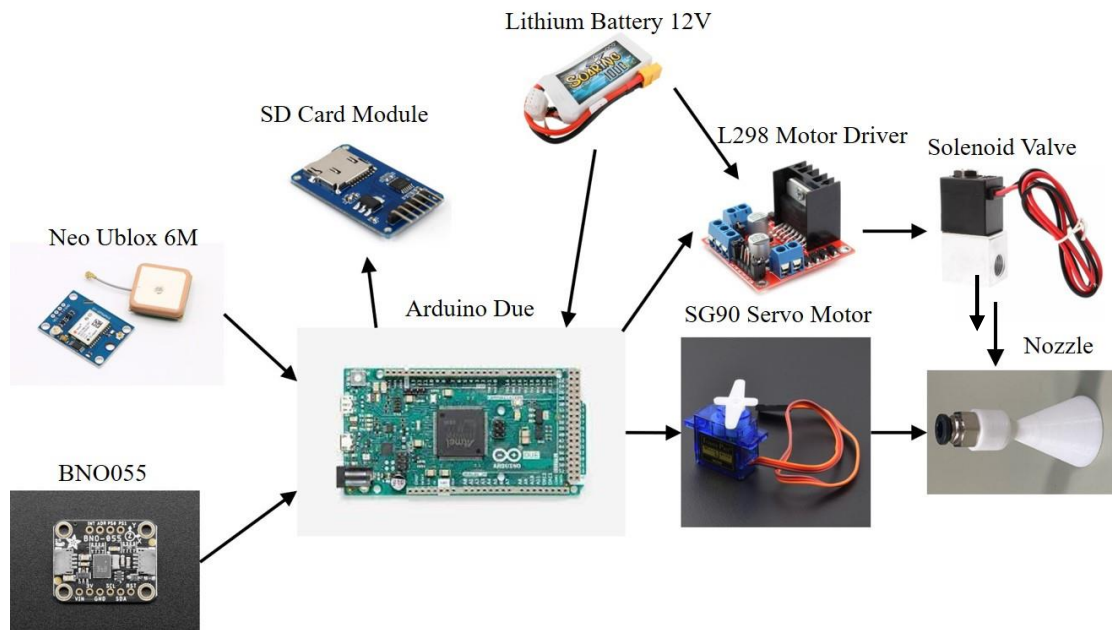
Figure 3.19

Finalize Nozzle Designs



Figure 3.20

Overall Electronics Components Connection



3.2.5 Tracking System Implementation

Since the trajectory tracking system is based on the GPS, it is important to obtain the position and heading degree data of the system. Since, the BNO055 can provide the compass data, the North direction can be obtained from this. The heading data, the angle data and desired GPS points are inserted into the Arduino Due to calculate. Since, the BNO055 is small and powerful IMU, but the magnetometer data obtained by the BNO is noisy and very unstable. To avoid this condition, the second order Butterworth low pass filter or Kalman's filter is used to cancel most unwanted noise data.

Butterworth low pass filter provides passband flatness to maximum so, it can be called anti-aliasing filter. The higher the order of the filter, the longer flatness the pass band will be. The general form of transfer function model of the second order Butterworth low pass filter can be described as:

$$H(s) = \frac{K}{s^2 + 2\xi\omega_n s + \omega_n^2},$$

where K = overall gain, ξ = damping of the system, ω_n = natural frequency

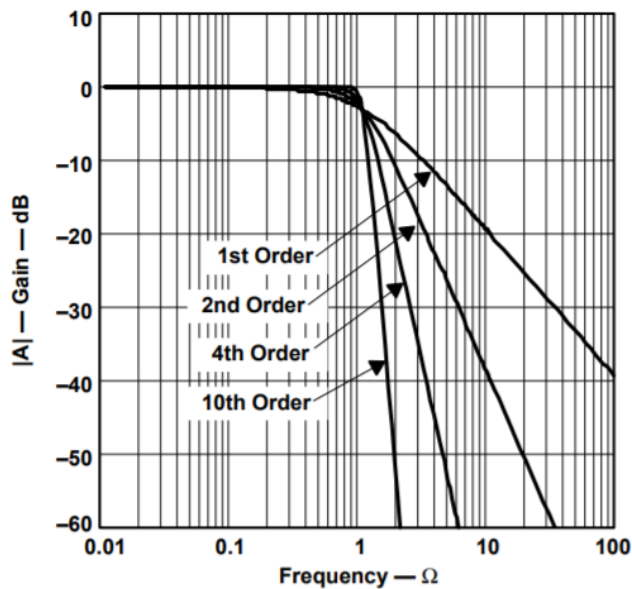
The polar form of the low pass filter is given by:

$$\left| \frac{\text{Output}}{\text{Input}} \right| = \frac{K}{\sqrt{1 + \left(\frac{f}{f_h} \right)^4}}$$

Where K = gain in pass band, f = input frequency, f_H = cutoff frequency

Figure 3.21

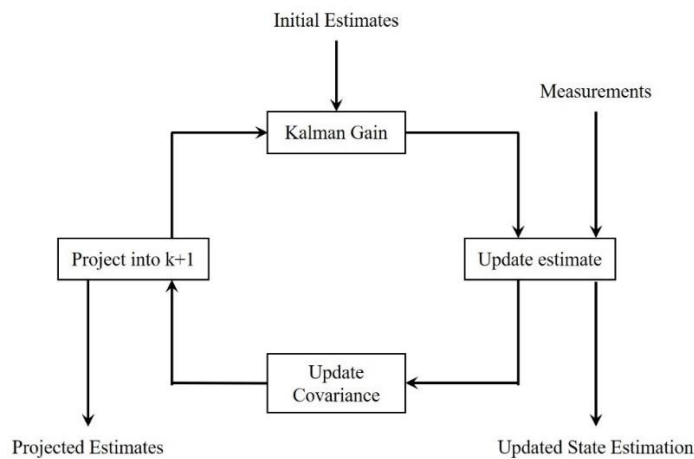
Response of Butterworth LPF According to the Orders



Another powerful and robust filter is the Kalman filter. It provides an optimal estimated sensor reading from the noisy measurements. Kalman filter is mutual estimation and one of the most essential filters. Estimation of hidden variables are produced based on imprecise and undefined measurements. Not only estimation of hidden variables, but also provides a prediction of the future system state based on these estimations.

Figure 3.22

Kalman Filter Algorithmic Loop



The following equations are used to implement the Kalman filter. But in this system, only 1DOF Kalman filter is implemented.

$$K = \frac{PH}{HPH + R} \quad (\text{update Kalman gain})$$

$$\hat{U} = \hat{U} + K[U - H\hat{U}]$$

$$P = (1 - KH)P + Q$$

For the variable, the following initial conditions are used.

$$\phi = 1.0, H = 1.0, R = \text{Con}(v) = 50, Q = \text{Con}(w) = 10, P_0 = 0, K_0 = 0$$

Also the GPS data are unreliable and the data obtained are really chaos, it also need a filter to obtain the GPS data with less noise. But, the GPS cannot get a data without a noise because it is controlled by the satellite owner and need more complex algorithms to get the exact location of the GPS. In case of that, low pass filter is enough in order to get the GPS data even though it is not a good result.

$$\frac{\text{Output}}{\text{Input}} = \frac{K}{\tau s + 1}$$

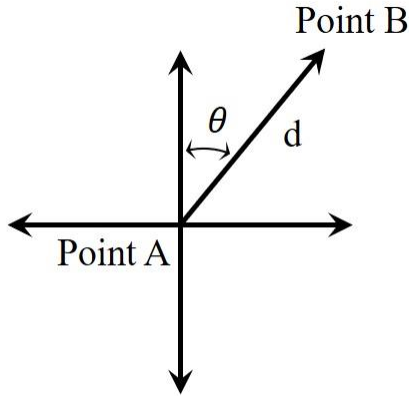
Where τ = time constant, K = gain

In order to make a rocket to go to the predefined location, the GPS navigation is needed to apply. GPS is the global positioning system that use radio receiver to collect signals from satellites to determine the one's position, speed and time. Distance represents the

shortest way between the two points. Bearing shows the angle between the current position and the desired destination.

Figure 3.23

Haversine Formula for Waypoint Tracking



The Haversine formula is used to get the bearing angle and distance between two GPS coordinates.

$$a = \sin^2(\Delta\varphi / 2) + \cos\varphi_1 \cdot \cos\varphi_2 \cdot \sin^2(\Delta\lambda / 2)$$

$$c = 2 \cdot \tan^{-1}(\sqrt{a} / \sqrt{1-a})$$

$$d = R \cdot c$$

The bearing angle between two points can be calculated from the formula:

$$\theta = \tan^{-1}(\sin\Delta\lambda \cdot \cos\varphi_2 / \cos\varphi_1 \cdot \sin\varphi_2 - \sin\varphi_1 \cdot \cos\varphi_2 \cdot \cos\Delta\lambda)$$

where φ is latitude, λ is longitude, R is earth's radius (6371 km), $\Delta\varphi$ is difference between two latitude points and $\Delta\lambda$ is difference between two longitude points.

To get the heading from the magnetometer, the following equations will be used. The magnetometer provides the 3DOF, and to get the 1DOF magnetometer data, the 3DOF data are gathered and then normalize to get the 1DOF again.

$normalizeMag = \sqrt{magX^2 + magY^2 + magZ^2}$, where magX, magY and magZ is the magnetic data obtained from the magnetometer.

$$normalizeX = \frac{magX}{normalizeMag}$$

$$normalizeY = \frac{magY}{normalizeMag}$$

$$headingDeg = \tan^{-1}\left(\frac{normY}{normX}\right) * \frac{180}{\pi}$$

But on the earth's surface, the compass does not show exactly to the north. There is a deviation from the true north and it is called declination angle or sometimes, magnetic declination. The declination angle is different according to the places. The declination angle of the Thailand is about 5.12 degree so, the finalize equation of the heading degree of the compass is:

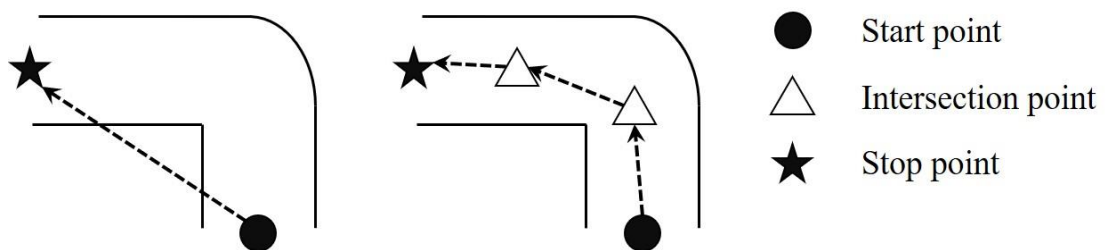
$$headingDeg = \tan^{-1}\left(\frac{normY}{normX}\right) * \frac{180}{\pi} + 5.12$$

To prevent turning under 0 or over 360, the heading degree is adding or subtracting 360 degree to avoid that situation. If heading degree is under 0, the 360 degree is added to the heading degree and over 360, the 360 degree is subtracted.

Going along with the waypoint is the essential for the target tracking system. The target point is the latitude and longitude and if the rocket has to turn left or right on the bending path, one point target system is not sufficient. In this case, more than 2 or 3 points are used to avoid only straight-line tracking.

Figure 3.24

Path Comparison Between with Direct Point and with Intersection Points



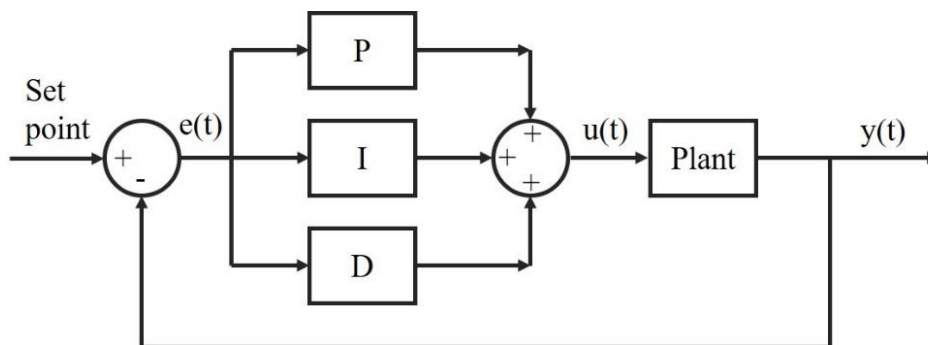
In figure 3.22, the left one is the one point target system. The tracking can be achieved but it'll deviate from the lane. As a result, it can go into the holes, or maybe grass lawns, or unwanted environments. To prevent this from happening, the points are given as shown in figure 3.22 on the right figure. When the rocket reaches to the near intersection point (<3 m), it'll shift to the another point automatically.

3.2.6 Conventional Proportional-Integral-Derivative Controller

Proportional-Integral-Derivative (PID) controller is the most commonly used control algorithm in control system. The PID controller is famous for its robustness in a variety of functioning systems. Beside it is very simple and easy to understand and implement. Theoretically, the PID controller is composed of three basic constants namely proportional, integral, and derivative. The Proportional value is concerning with the current error, the Integral affects the response based on the total error of recent and the Derivative regards with the response to the error changing rate. The sum of these three terms is used to modify the process to get the robustness. The main function of PID controller is to continuous calculating of an error value as the changes between a determined point and calculated actual value and then, utilizes a adjustment based on proportional, integral, and derivative gains.

Figure 3.25

Block Diagram for PID Controller



The proportional term “P” rely on the current error, the subtraction between the desired value and acutal value. The speed of the control response will be increased together with the gain “P” increment but, too large “P” value can make the system oscillate.

The output of the proportional control is,

$$u(t) = K_p e(t)$$

The integral term “I” is the sums of the error terms over the time. The small error term will produce the integral part to rise slowly. Until the error becomes zero, the “I” will increase along with the time continuously to get steady state to zero.

The output of the Integral control is,

$$u(t) = K_i \int e(t) dt$$

The derivative term “D” is the change of the process variable regarding with the time. By increasing the “D” term, it will affect the control system to react more to changes in the error. And it also increases the rate of the control response. Small “D” value is used in most real control systems because it is highly responsive to noise in the system. The output of the Derivative control is,

$$u(t) = K_d \frac{de(t)}{dt}$$

The mathematical expression of the PID controller is,

$$u(t) = K_p e(t) + K_i \int e(t) dt + K_d \frac{de(t)}{dt}$$

To get the system stability and robustness, the parameters of the PID are needed to be tuned optimally. Gain tuning is the important factor for all closed-loop control systems. The most famous PID tuning techniques are trial-and-error method and Zeigler-Nichols Tuning method. The first method (Trial-and-error) is the simplest of PID tuning methods. The gain parameters of PID are adjusted manually. The gain parameters are tuned by looking the system’s behaviors during the experiments until the best performance is obtained. When “P” response is sufficient, integral term is secondly needed to be handle, then the fluctuations of the system will be decreased. Until the steady state error is decreased, adjust the “I” term. but it can increase overshoot. After “P” and “I” parameters have been tuned to a desired value with slight steady state error, adjust the derivative gain up to the system responds quickly to its desired point.

Table 3.10

Effects of Increasing PID Parameters

Control Response	Settling Time	Overshoot	Steady State Error
Increasing K_p	Minimal Impact	Increases	Decrease
Increasing K_i	Increases	Increases	Zero steady-state error
Increasing K_d	Decreases	Decreases	No impact

3.2.7 Control Implementation

The control procedure of the autopilot system of the missile in this thesis can be seen in flow chart as shown in figure 3.24. Firstly, the desired latitude and longitude data are given advanced and as soon as the GPS signal is online, the process begins. There are two main steps to reach to destination point, checking whether the rocket heading is equal to the desired heading and whether it reach to the desired position or not. If the heading is off from the desired heading, the servo motor which is used to control the movement of rocket nozzle, will rotate to adjust to reach to the desired yaw angle.

After that, the air will be supplied continuously until it reached to the desired location. As two or more waypoints may be included, it will be checked until there are no more waypoints left to be processed. The system included PID loop which is intended to achieve the robust tracking process for the rocket to get to desire position. The heading error can be calculated as follow:

$$\textit{headingError} = \textit{bearing} - \textit{headingDeg}$$

But the rocket is originally intended to control heading values between -180 to +180, so, the 360 is added to the heading error.

$$\textit{headingError} > 180, \textit{headingError} - = 360$$

$$\textit{headingError} < -180, \textit{headingError} + = 360$$

The output heading error is then passed into the PID control block and the output yaw is obtained after processing with the PID. Preventing from going over 360 or under -360 degree, the output yaw control is added or subtracted from 360 degree if the output yaw value exceeds 360 or gets lower than -360.

Figure 3.26

Overall Block Diagram of the Autopilot System

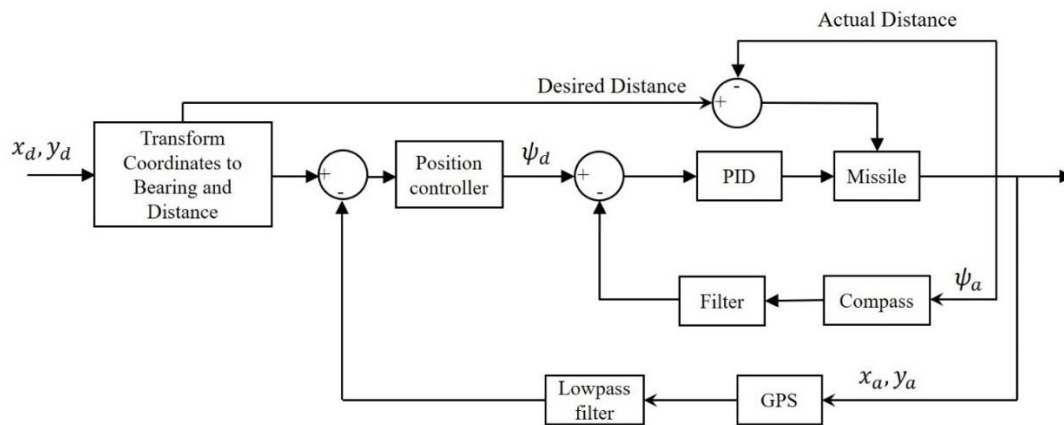
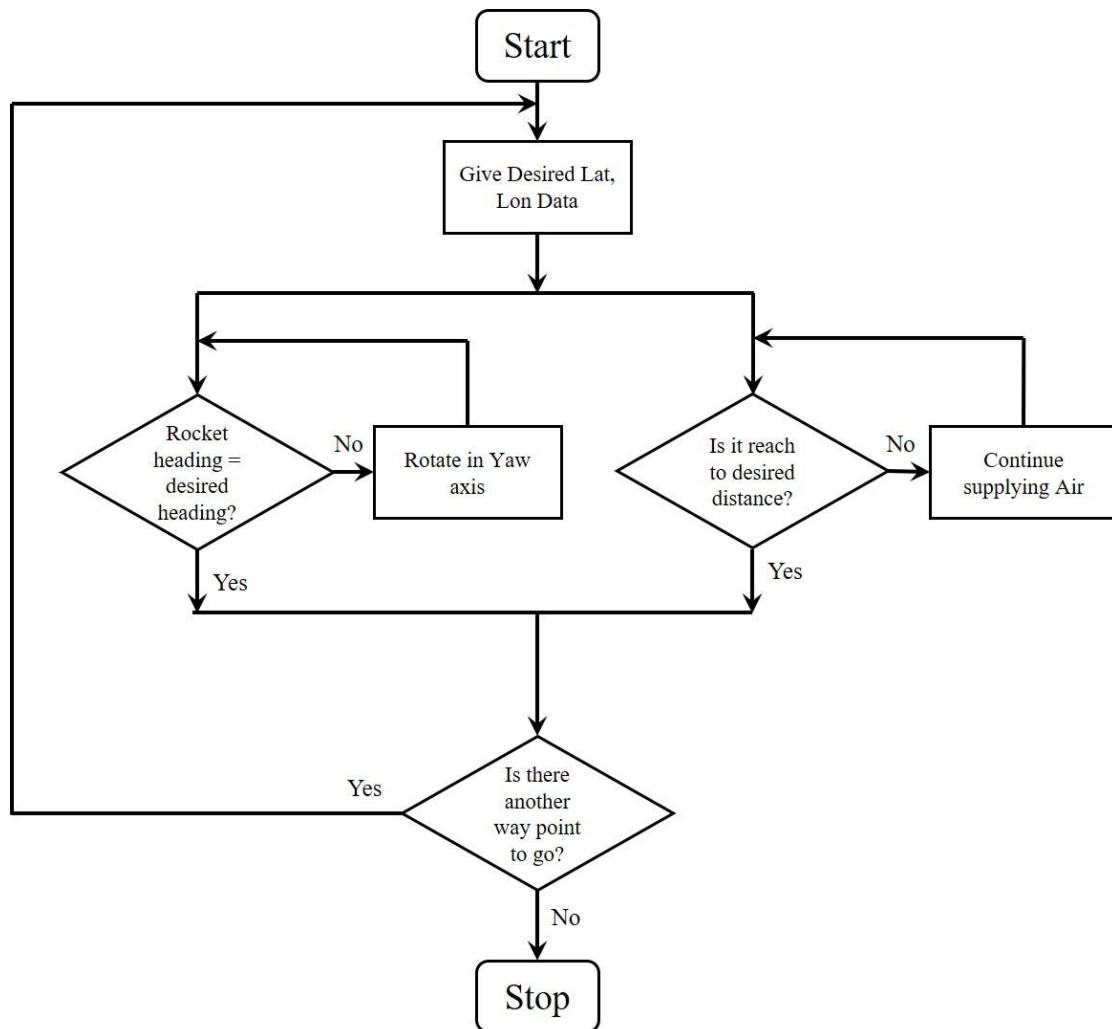


Figure 3.27

Flowchart of the System



3.3 Water Rocket

3.3.1 Water Rocket Concepts

Newton's first law and Newton's second law and Newton's third law are acted upon the all kind of missiles.

Newton's first law is that objects which are staying at the rest position will stay at rest, or the objects which are in motion condition will stay in motion until there are unusual external force acting upon them. At the time the rocket is placing on the rocket launcher, the forces are balanced because of the rocket is pulled up the the launcher while the gravity pulls it down. When the compressed fluid inside the water rocket bottle was released by opening the locking clamps the forces become unstable and the compressed fluid is ejected from the small opening at the bottom of the rocket. This provides the thrust and allowing the rocket to go upright.

Newton's second law is that the object's acceleration is directly proportional to the force acting on the object and inversely proportional to the mass of the object. So, to fly the rocket to good heights, minimizing the rocket's weight and on the other hand increasing the thrust force. But as for the caution, if the rocket body is so light, it might affect the stability after the water is ejected and it will flip over. The larger mass of fluid and the quicker the fluid can be ejected from the rocket, the more thrust force it can be produced.

Newton's third law is that for every action and consequences, there is always an opposite and equal reactions. As soon as the clamp lock is released, the compressed fluid escapes the bottle which provides the action force that is come with equal and opposite reaction force. This leads the rocket to go opposite directions.

3.3.2 Takeoff Early State Calculation

The net axial force of the water rocket on the rocket launcher is:

$F_{rod} = (P - P_{atm})A_e$, where A_e is cross sectional area of the nozzle, P is compressed air pressure in the bottle, P_{atm} is atmosphere pressure.

Thrust force equation of the water rocket is $F_{thrust} = \dot{m}u_{ex} = \rho_w A_e u_e^2$ where ρ_w is water density, u_e is the exhaust velocity of the rocket. Exit velocity of the water rocket can be obtained from:

$$u_{ex} = \sqrt{\frac{2(P - P_{atm})}{\rho_w}}.$$

Thus, the thrust force can be known as

$$F_{thrust} = 2(P - P_{atm})A_e.$$

The drag force can slow down the rocket's movement in the air. The drag force depends on the air's density, speed of the rocket and cross-sectional area and drag coefficient. The drag coefficient (C_D) is different from medium object to object, 1.0 for non-streamlined objects and 0.1 for very streamlined objects.

The drag force can be expressed as

$$F_D = -\frac{1}{2}\rho_{air}C_D A_R.$$

Thus the forces acting on the body can be expressed as

$$F_{total} = F_{thrust} + F_D - mg.$$

Figure 3.26 shows the water rocket simulation made by Clifford Heath. By varying the rocket volume, water volume, pressure, nozzle size, bottle diameter, drag coefficient, dry mass (without water), and if the water rocket is the two-stage rocket, the initial speed for second stage can be added, and length of the lunch tube and diameter. As the results, the thrust phase, burnout, coast, crash down data as well as altitude graph, speed graph, acceleration graph and thrust graph can be obtained.

Figure 3.28

Water Rocket Simulation From <http://polyplex.org/rockets/simulation>

Water Rocket Simulation [Home Page](#)

This page does a numerical simulation of the entire flight of your rocket. Just enter the details below, and see how your rocket flies!

Now including Bruce Berggren's air pulse formula! The air pulse is taken as an instantaneous impulse, so the acceleration curves don't show it, but the velocity curve takes a jump upwards on burnout.

Also with Launch Tube simulation, including the ability to use a launch tube of a different size from the nozzle, like with Scott's T-Nozzles.

Rocket volume:	2	(litres)
Water volume:	0.6	* (litres)
Pressure:	120p	(in Kpa, append 'b' for bars, 'p' for PSI)
Nozzle size:	22	* (millimeters)
Nozzle loss factor:	0.16	* (0.05-0.3ish)
Bottle diameter:	110	(millimeters)
Coefficient of Drag:	0.3	(typical range 0.1-0.5)
Dry mass:	100	* (grams)
Initial speed (for second stage):	0	(metres/second)
Launch tube length:	0	(millimetres)
Launch tube diameter:	0	(millimetres, zero means same as nozzle)
Water density:	1	* (kg/litre)

Notes

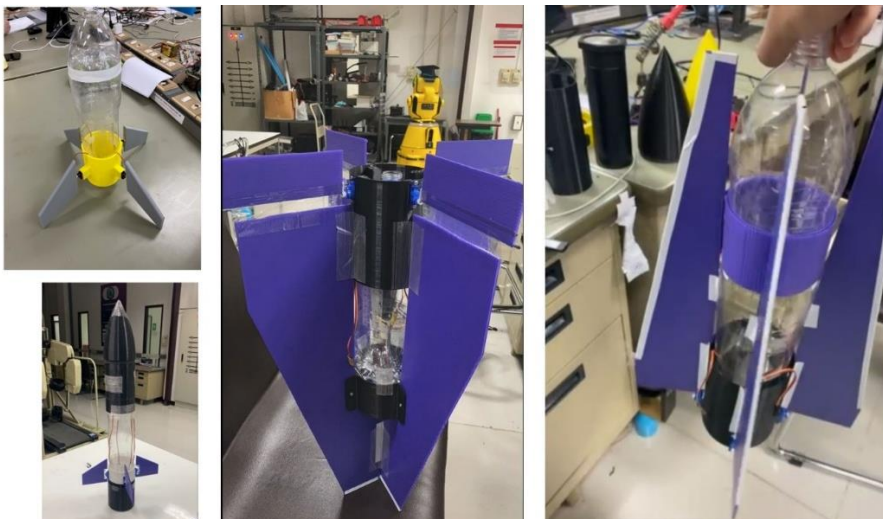
- Any single entry may be specified as a range, for example "80-120". This will divide the range into 20 (logarithmic) steps, and compute the simulation for all of the values. This suppresses the graph.
- A range specification for an entry marked with a * will show the best altitude achieved.

[Clifford's Home Page](#)

3.3.3 Hardware for Water Rocket

Figure 3.29

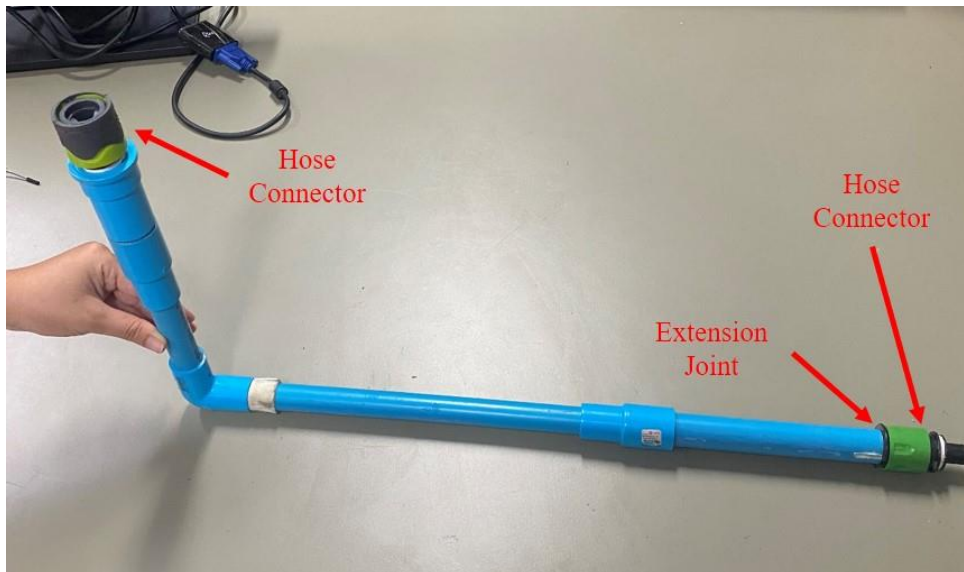
Water Rocket Models



For the launch tube, it is included the PVC pipe, and the hose connector which is used in the garden watering. The figure 3.27 shows the launcher design that is used. This style is influenced by the typical water rocket launcher.

Figure 3.30

Water Rocket Launcher



For the nozzle, the 9mm nozzle size is used for the thrust nozzle. The procedure of pressuring the water rocket is that firstly, the glued capped tap connector is connected to the hose connector. The pressure is compressed through the PVC pipe and then it is ready to release from the launcher.

Figure 3.31

Water Rocket Launcher



CHAPTER 4

RESULTS AND DISCUSSION

In this section, the results that have done on this thesis are shown. There are two parts, the first one is trying to make it fly but failed. The another one is moving on the ground with the free wheel like flying in the air.

4.1 Creating Thrust Force for Flying

To make a rocket fly in the rocket, the propulsion system is needed. There are two types of propulsion, solid fuel-oxidizer mixture propellant and liquid propellant which is used with the liquid fuel and oxidizer, combine them to produce thrust force. Figure 4.1 shows the solid rocket motor firstly intended to use but because of its high flammability, the idea of using it is cancelled. It contained 60% of potassium nitrate, 30% of sugar and 10% of corn syrup. It is typically known as sugar rocket motor.

Figure 4.1

Sugar Rocket Prototype



4.2 Water Rocket Analysis

4.2.1 Water Rocket Simulation Analysis

The following table 4.1 shows the data that are used in the water rocket simulation from the website <http://polyplex.org/rockets/simulation/>

The important factor for adding the water to the water rocket is that the volume water should be one-third ratio of the rocket volume. If it is lower than that, the thrust force will be decreased. If it is higher than that, it will turn over and the thrust force can not lift the water rocket.

Table 4.1

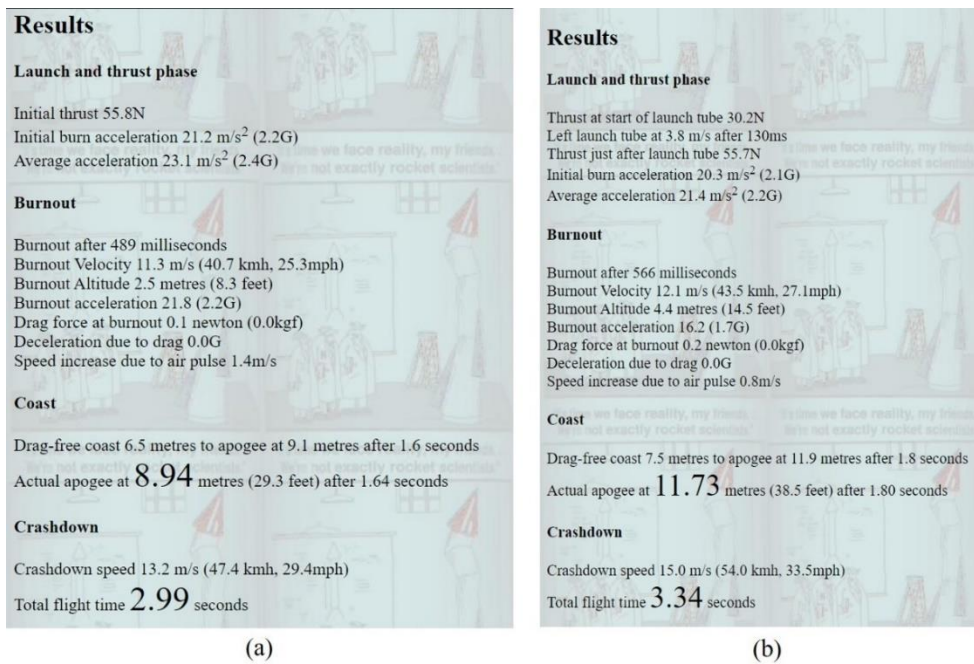
Parameters for Water Rocket Simulation

Specification	Test (1)	Test (2)
Rocket Volume	2.75 L	2 L
Water Volume	0.9 L	0.7 L
Pressure	500000.00 Pa	500000.00 Pa
Nozzle Size	9mm	9mm
Bottle Diameter	110mm	110mm
Dry Mass (Without Water Mass)	1150	1150
Launch Tube Length	1000	1000

Figure 4.2 and figure 4.3 are the results and graphs for the water rocket simulation. As for the simulation test, the different two bottles are tested. Bottle number (1) is 2.75 liter bottle which is connected two cut bottles and another bottle number (2) is the 2 liter Coca-Cola bottle.

Figure 4.2

Water Rocket Simulation Results (a) Bottle (1) and (b) Bottle (2)

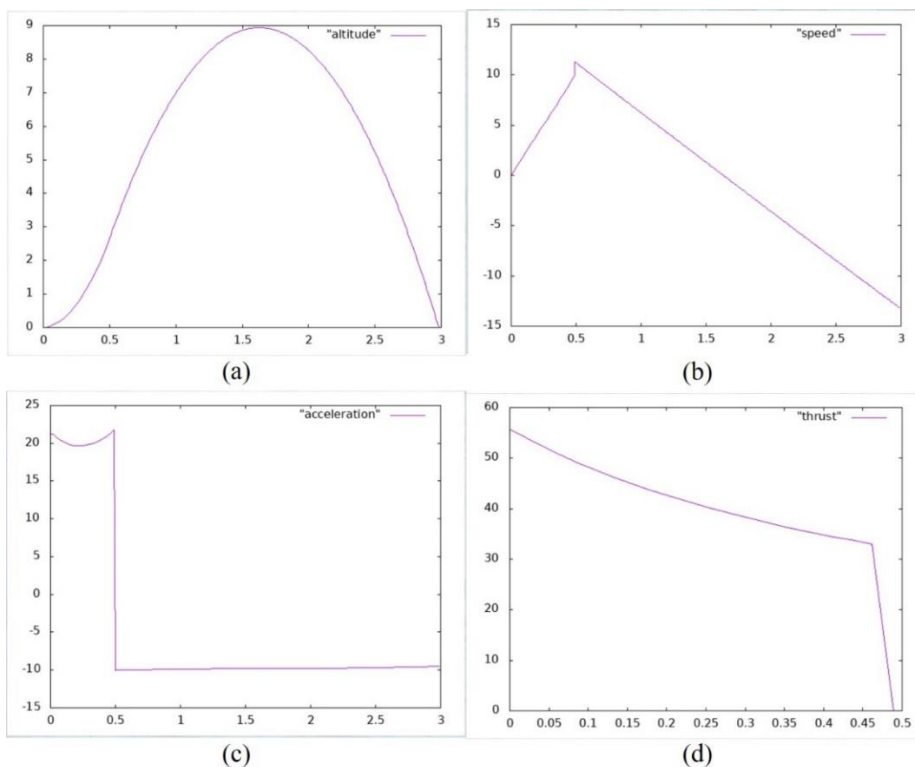


(a)

(b)

Figure 4.3

Bottle (1) Graph for (a) Altitude (b) Speed (c) Acceleration (d) Thrust



(a)

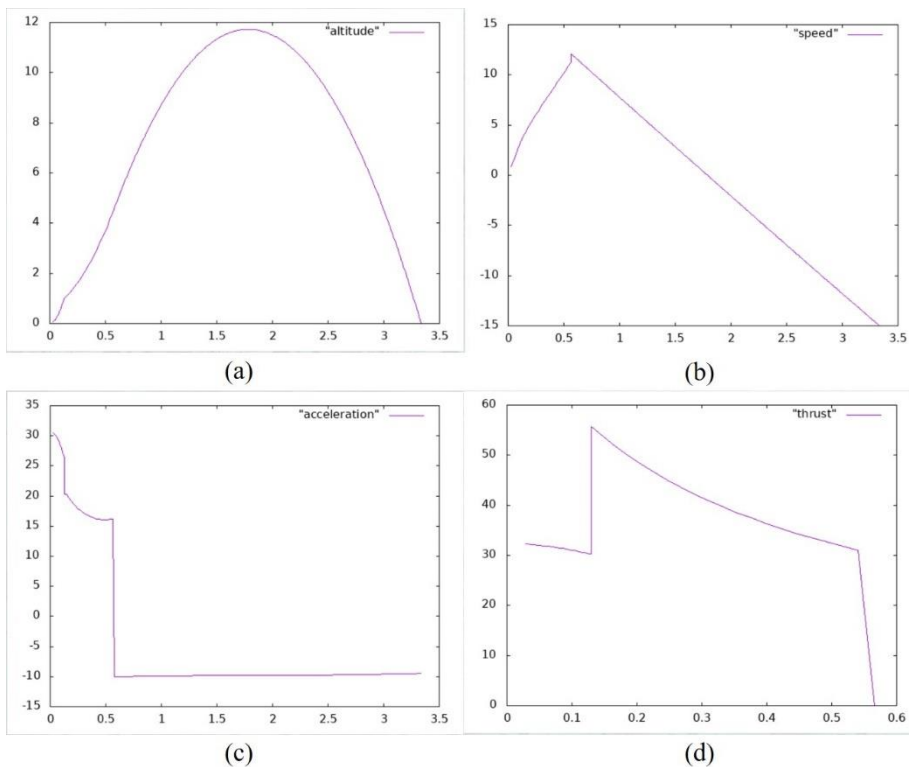
(b)

(c)

(d)

Figure 4.4

Bottle (2) Graph for (a) Altitude (b) Speed (c) Acceleration (d) Thrust



The water rocket is the most basic of the high school project. The result of the water rocket looks promise, but it cannot hold the airtime so much longer. At least, more than 30 seconds is needed to maintain the control system works perfectly. But with the lack of soft landing when the water rocket got back to the ground and the ground was really hard because of the hot weather, the water rocket was broken. To increase the volume of the rocket propulsion, the silicon was used to connect between two cut bottles. But, if the air pressure was inserted more than 400,000 psi, the joint between these bottles which were connected with the silicon was disconnected and it tended to system failure.

4.3 Results of Computational Fluid Dynamics Analysis (CFD) on Nozzle

The computational fluid dynamics analysis (CFD analysis) is used to analyze the velocity and pressure of the nozzle. By using CFD, one can analyze sophisticated problems that is concerned with fluid-fluid, fluid-solid or fluid-gas collaboration. CFD analysis have a great benefit on saving time in the design development so, it is cheap and fast compared to typical testing for data collecting upon the prototype.

Figure 4.5

Water Bottle Rocket Failures

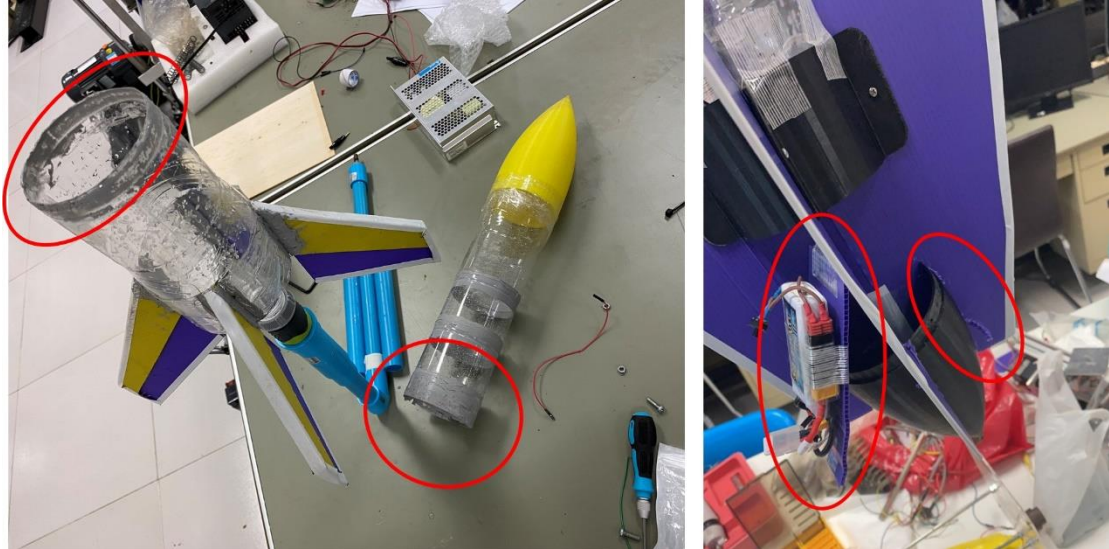


Table 4.3 shows the specification of the nozzle (1) that is analyzed. For this nozzle, all of the dimensions are given without proper calculations and making the exit radius is 10 times bigger than the throat radius. The prototypes are designed in the Solidworks software and CFD analysis is also operated in the Solidworks. The figure 4.4 represents the nozzle prototype with the dimensions.

Table 4.2

Modeling Geometry of Nozzle (1)

Properties	Values
Inlet radius	6.5 (mm)
Throat radius	1.55 (mm)
Exit radius	15 (mm)
Thickness	1.5 (mm)
Length of chamber	12 (mm)
Length of nozzle	35.1 (mm)

Figure 4.6

Nozzle(1) Dimensions

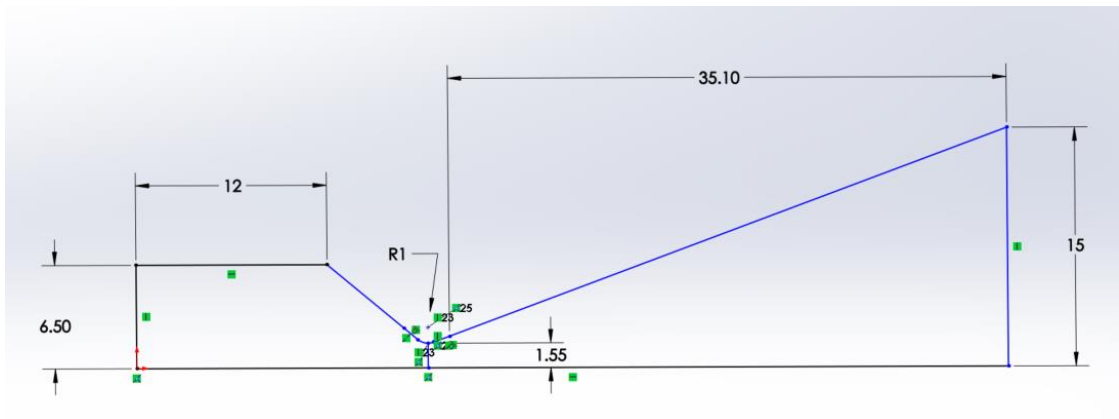
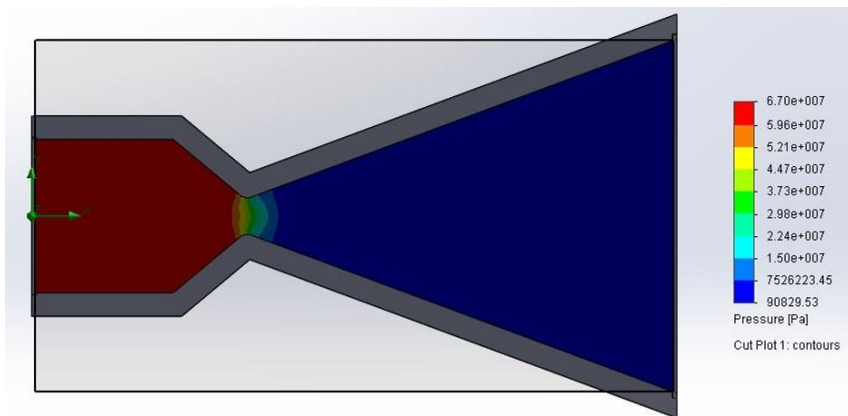
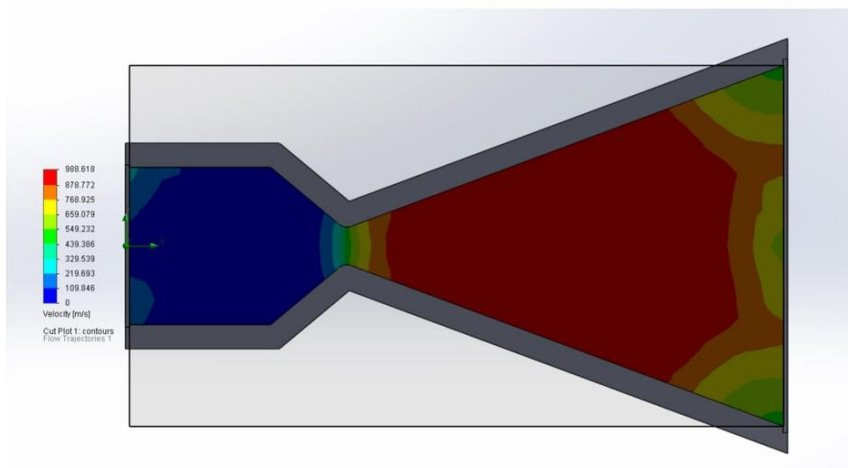


Figure 4.7

CFD Analysis of Nozzle (1) Showing (a) Pressure Cut Plots and (b) Velocity Cut Plots



(a)



(b)

Table 4.4 shows the specification of the nozzle (2) that is analyzed. For the second nozzle, the dimensions are calculated with the design equations to obtain the 5N thrust force, then constructed in Solidworks and analyzed.

Table 4.3

Modeling Geometry of Nozzle (2)

Properties	Values
Inlet radius	6.5 (mm)
Throat radius	2.5 (mm)
Exit radius	5.95 (mm)
Thickness	1.5 (mm)
Length of chamber	40 (mm)
Length of nozzle	20.28 (mm)

Figure 4.8

Nozzle(2) Dimensions

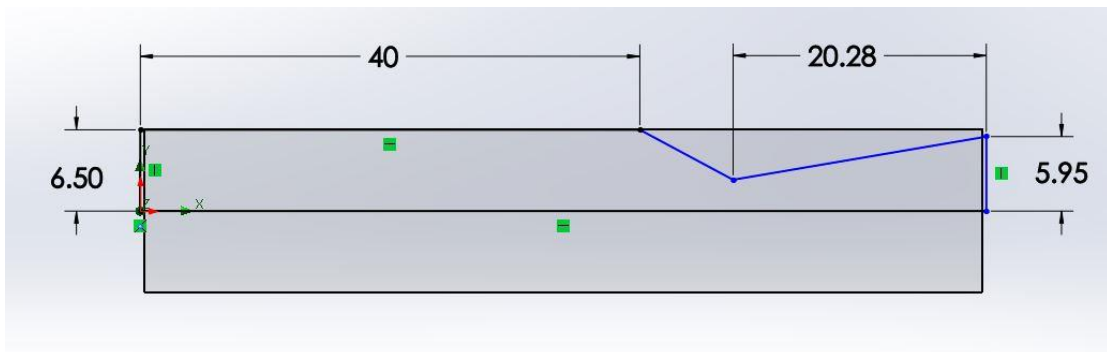
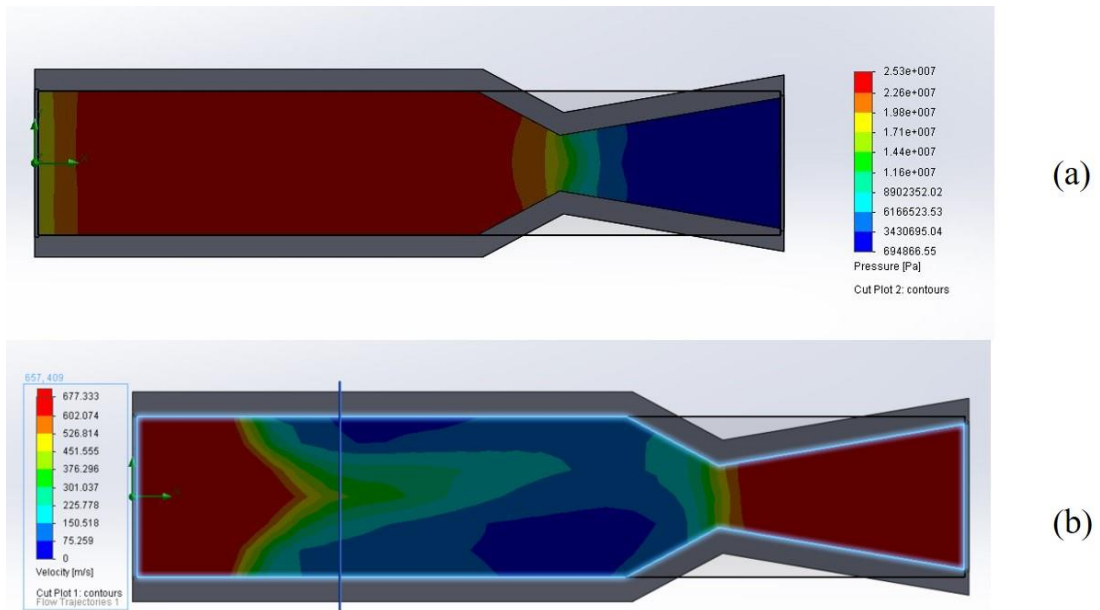


Figure 4.9

CFD Analysis of Nozzle (2) Showing (a) Pressure Cut Plots and (b) Velocity Cut Plots



The velocity and pressure outputs of the nozzle (1) and nozzle (2) can be seen in Table 4.5.

Table 4.4

Velocity and Pressure Comparison Between Two Nozzles

Nozzle Number	Properties	Values
1	Exit velocity	550 ~ 878 (m/s)
	Exit pressure	90829 (Pa)
2	Exit velocity	602 ~ 677 (m/s)
	Exit pressure	694866 (Pa)

4.3.1 Fluid Properties

The CFD analysis is carried out based on the Air as the operating fluid. The property of air is given in table 4.5.

Table 4.5

Specification of Air

Properties	Air
Density (ρ)	1.1644 (kg / m^3)
Gas constant (R)	287 ($J / kg.K$)
Specific heat ratio (γ)	1.4
Specific volume	0.814 (kg / m^3)
Pressure	101325 (kN / m^2)
Temperature	313 (K)

To accumulate the CFD analysis for both nozzles, the boundary conditions shown in table 4.6 are used. The inlet conditions are coming from the pressure pipeline from the lab. The environmental conditions are at atmospheric level.

Table 4.6

Specification of Boundary Conditions

Properties	Values
Inlet pressure	550,000 (Pa)
Inlet temperature	323 (K)
Inlet velocity	957 (m / s)
Atmospheric Pressure	101.325 (kN / m^2)
Atmospheric temperature	313 (K)

4.4 Experimental Analysis Between Two Nozzle Thrust Force

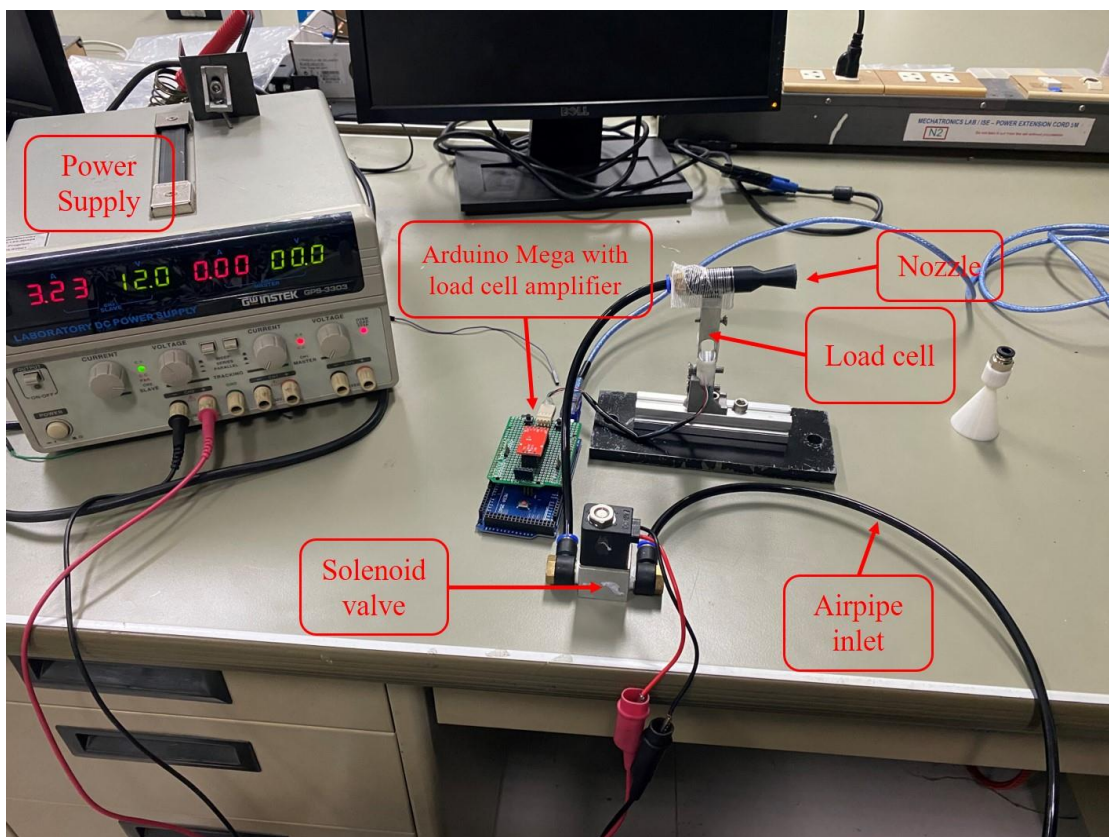
Since the thrust force is the important factor to drive the system, it is important to know the experiment for two nozzles which one can produce more thrust force. In an experimental setup, the main important tool is load cell with amplifier. The load cell amplifier is connected to the arduino. The data obtained from the load cell is the gram and to get the thrust force, the output data needs to be multiplied with gravity term 9.81 and since it is gram and thrust force is based on kg, it is divided by 1000.

The equation for the thrust force is:

$$T = \frac{\text{outputData} * 9.81}{1000}$$

Figure 4.10

Experimental Setup for Thrust Analysing

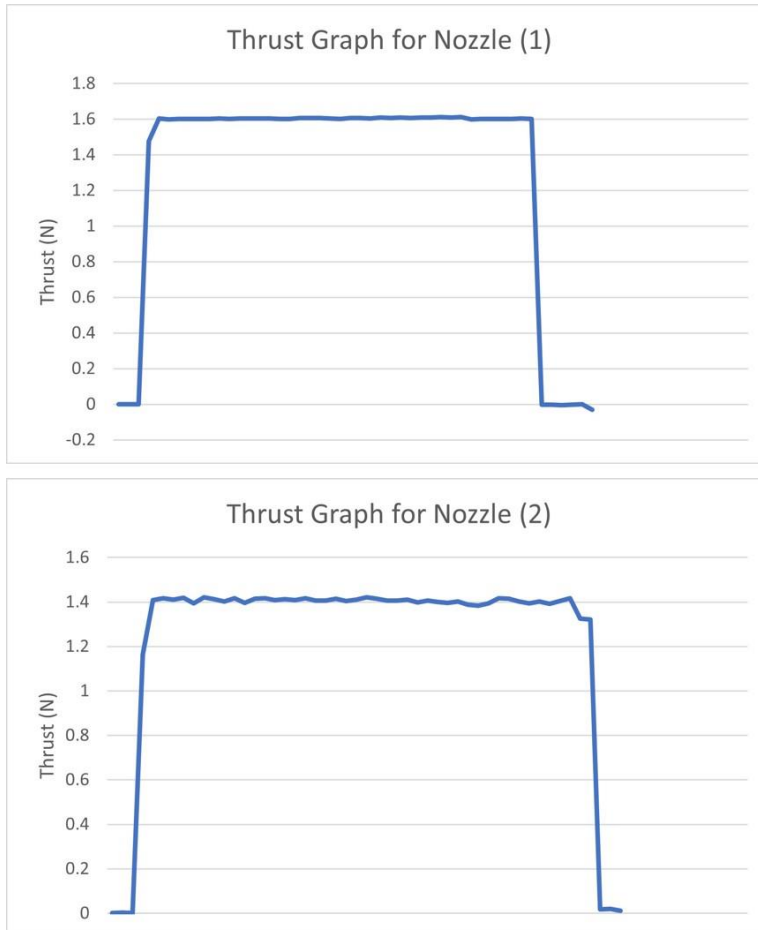


From figure 4.11, the nozzle (1) can produce 0.2 more thrust force than the nozzle (2). The more thrust force the system gained, the smoother the system can operate. So, in

this matter, the nozzle (1) is selected as the primary nozzle for the rocket propulsion system.

Figure 4.11

The Thrust Comparison Between Two Nozzle



4.5 Experimental Environment

The pressurized air flow is most important engine for making the thrust system. To get the good air flow, the air line from the mechatronics lab is used. Only using one air line is not enough air flow to move the rocket body, so in spite of using one airline, three airline is used to give enough air flow. The experiment is making outside of the mechatronics lab.

Figure 4.12

The Air Outlets from Mechatronics Lab



4.6 Comparison Between 2nd Order Butterworth Filter and Kalman Filter

In this experiment, the random magnetometer data is given to the filter to determine which filter is suitable for the system. In this case, the gains of the filters are not changing because this is intended to determine which one is better in any situation. By watching figure 4.1, it cannot be said which one is suitable for using in the heading calculation. In this case, root mean square error is used to determine which one is better.

Table 4.7

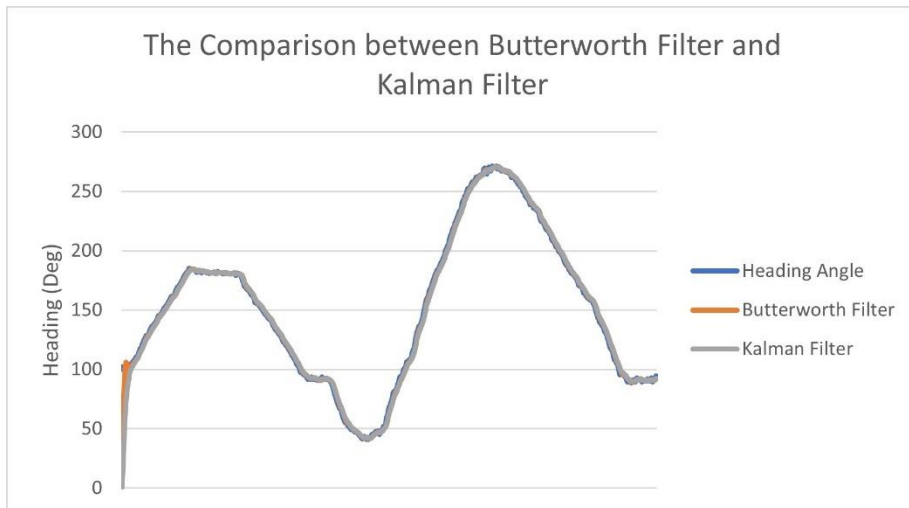
Root Mean Square Error for Comparison Between Two Filters

Filter name	RMSE value (Deg)
Butterworth	3.804862913
Kalman	4.553560517

By studying the table 4.7, it can be said that using Butterworth filter can give the better result than using Kalman filter.

Figure 4.13

Comparison Between Two Filters for Magnetometer's Heading Data

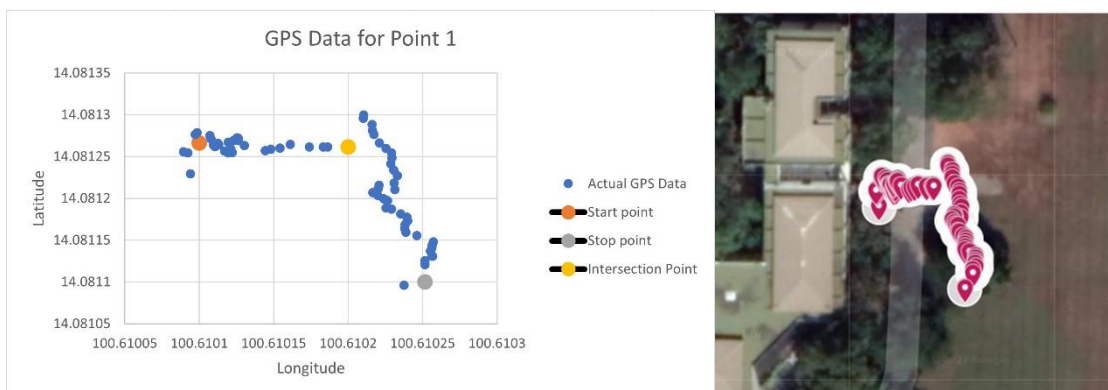


4.7 GPS Point Tracking

For GPS tracking, 5 waypoints are used to test its accuracy. In these experiments, the waypoints given are just the outside of the mechatronics lab room. To give the enough air flow rate, the air line from mechatronics lab is used. Due to the rocket to move outside of the lab, it need a long air supply and good flow rate so it can maintain the good thrust force. It can not go further than around 30 meters outside of the lab because of its long air pipe to supply air and prevent from dropping the flow rate.

Figure 4.14

GPS Coordinates for Point 1



From figure 4.14, the orange point is the start point where the rocket locates. The gray point is the stop point where the rocket needs to be stop. The blue data is the points along the path that the rocket goes toward the points.

As from figure 4.15, as it is reach to the next check point, the GPS algorithms take another point and then it is continuing to operate the tracking until it approaches to the 0 or nearly 0.

Figure 4.15

Yaw and Distance Error for Point 1

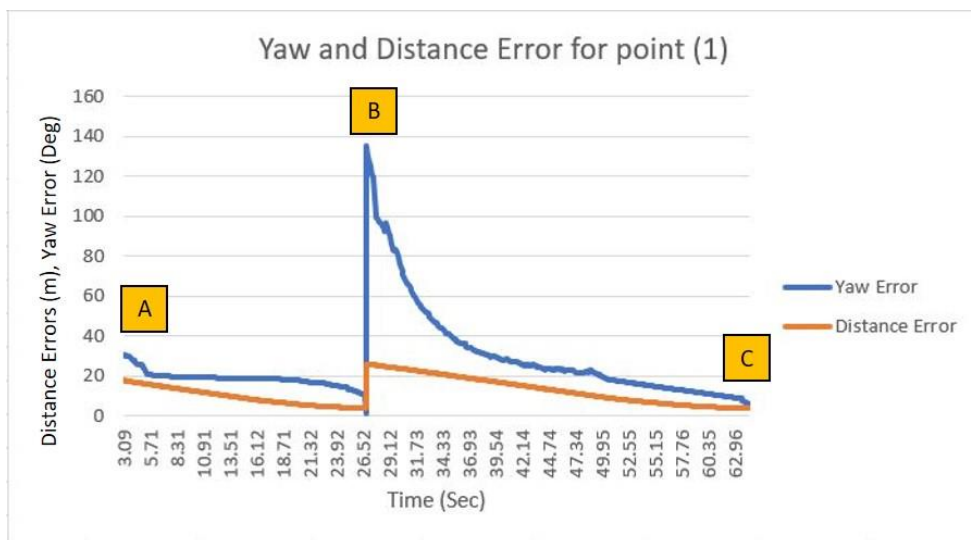


Figure 4.16

GPS Coordinates for Point 2

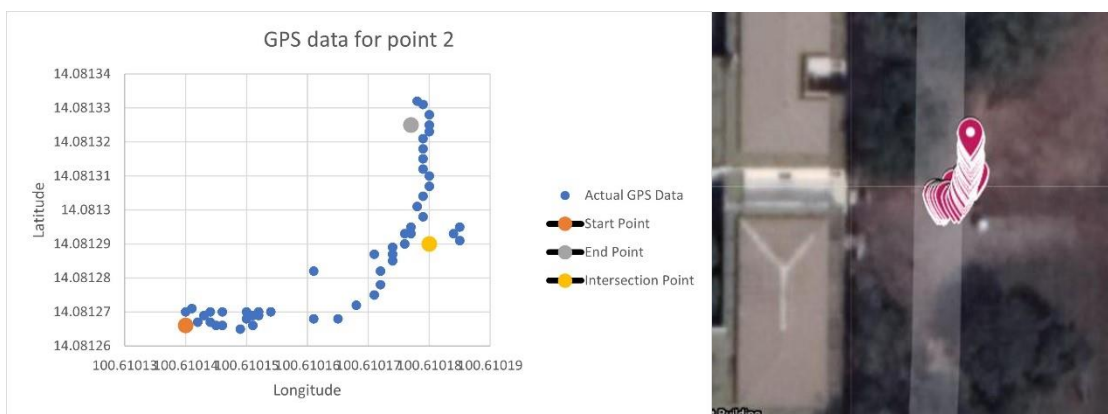


Figure 4.17

Yaw and Distance Error for Point 2

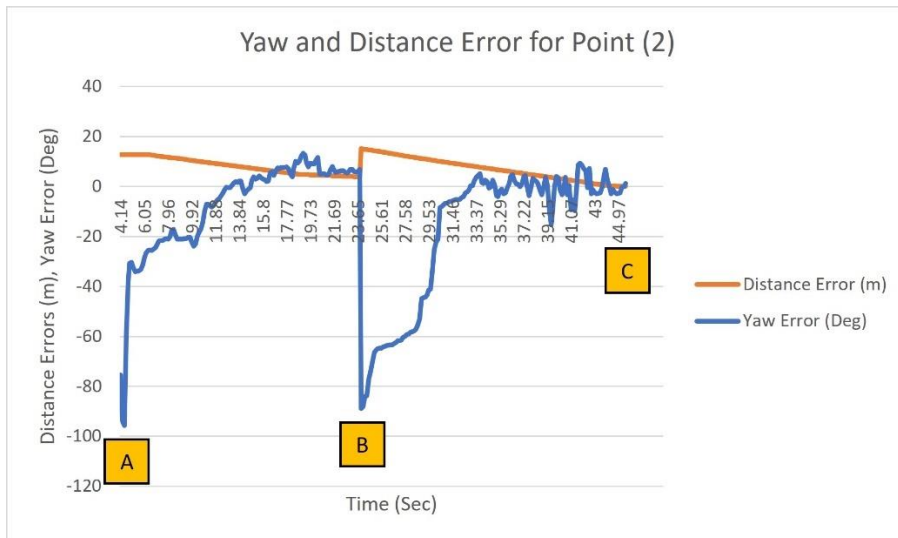


Figure 4.18

GPS Coordinates for Point 3

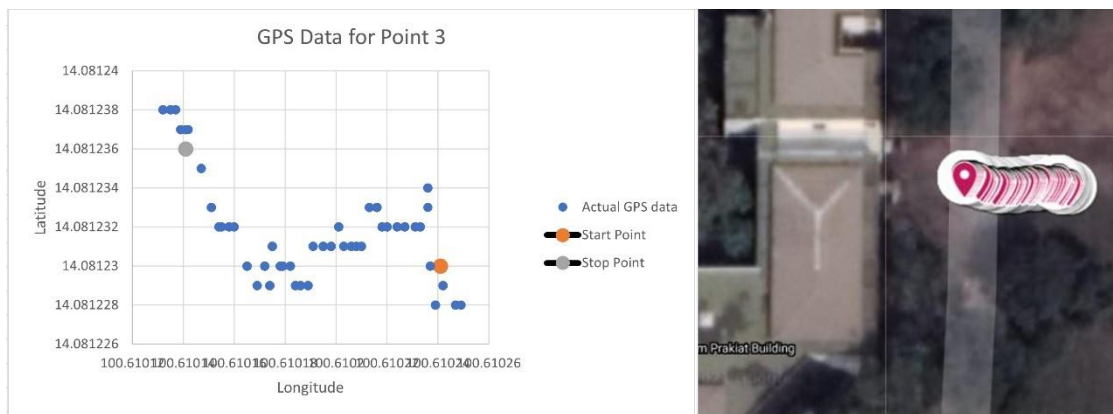


Figure 4.19

Yaw and Distance Error for Point 3

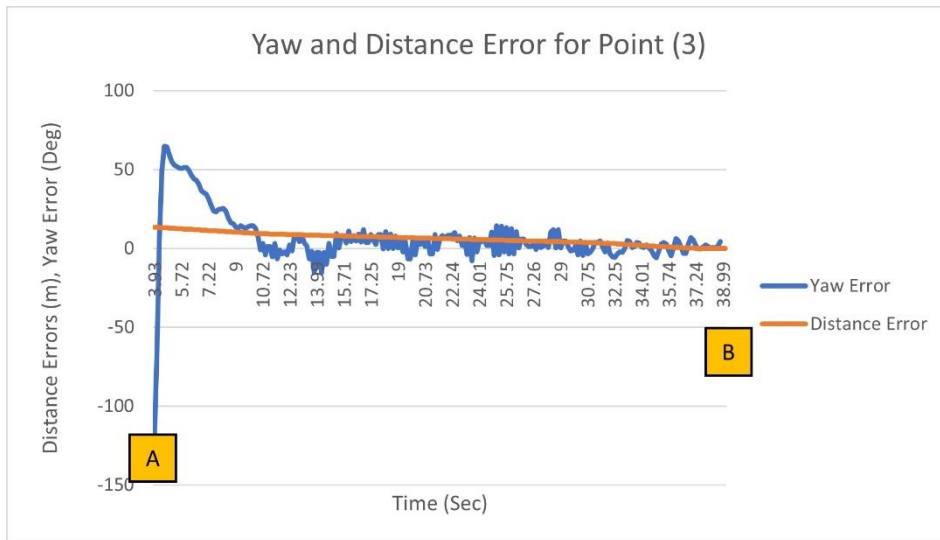


Figure 4.20

GPS Coordinates for Point 4

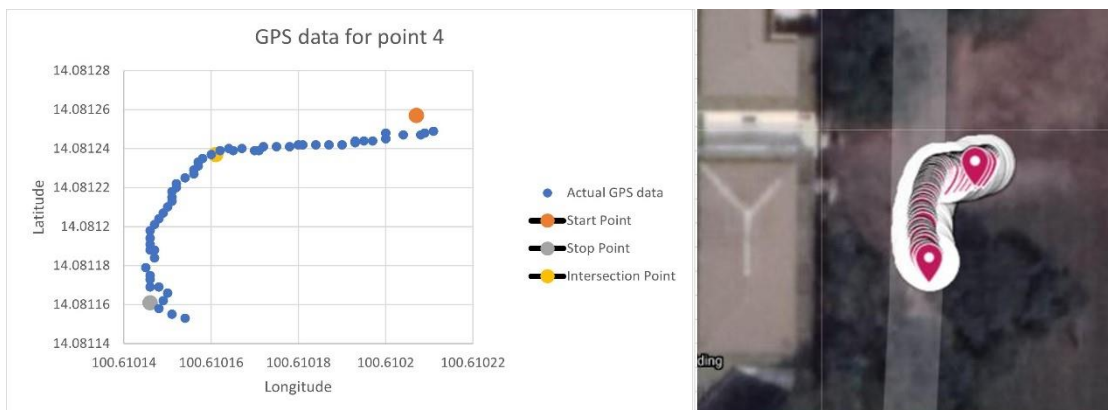


Figure 4.21

Yaw and Distance Error for Point 4

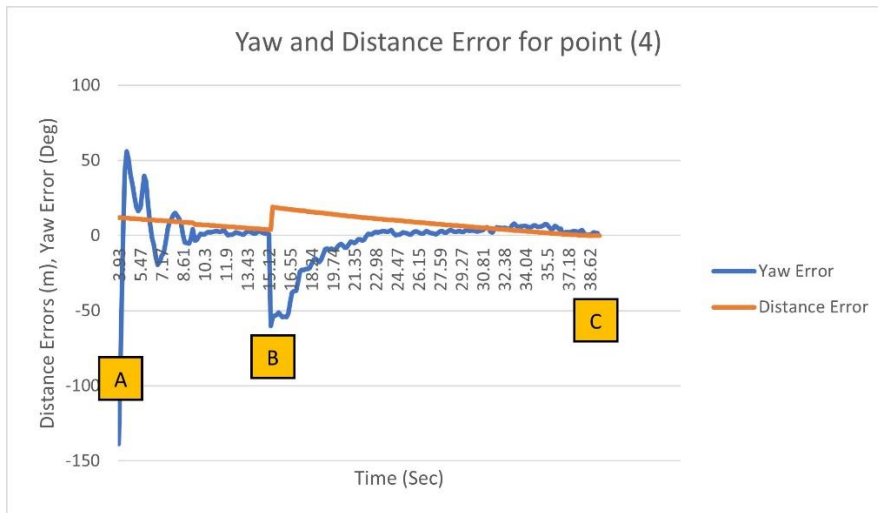


Figure 4.22

GPS Coordinates for Point 5

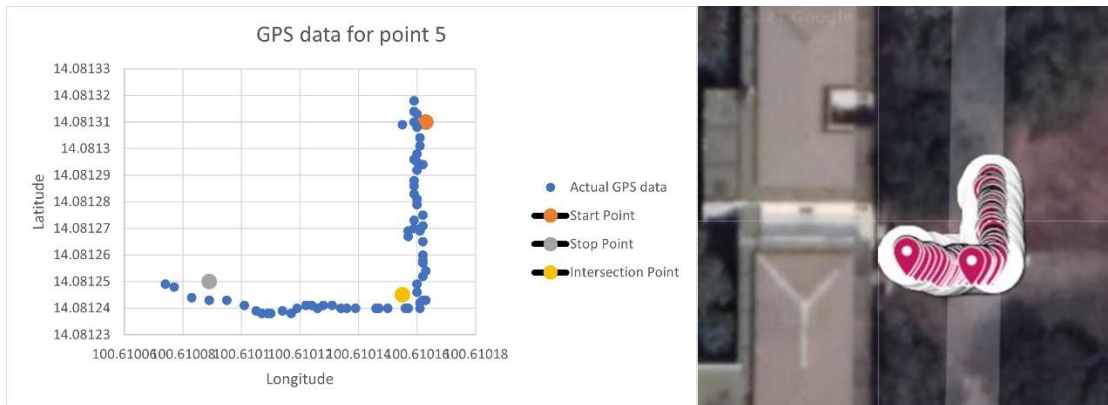


Figure 4.23

Yaw and Distance Error for Point 5

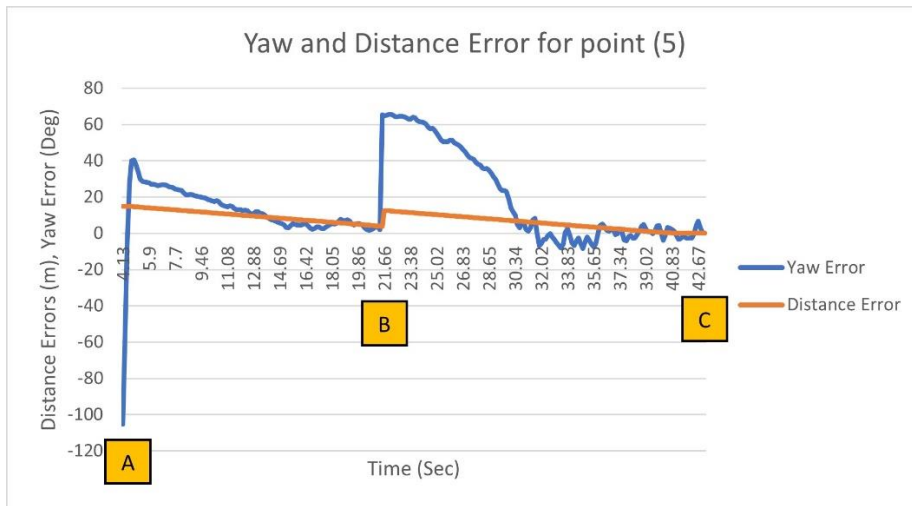


Table 4.8

Root Mean Square Error of Distance and Yaw for GPS 5 Points

GPS Points	Distance Error (m)	Yaw Error (Deg)
Point (1)	0.76053	4.012066
Point (2)	0.304138	2.721964
Point (3)	0.312018	1.594275
Point (4)	0.619275	5.965347
Point (5)	0.579562	4.372790
RMSE	0.5151046	3.7332884

CHAPTER 5

CONCLUSION AND RECOMMENDATION

5.1 Conclusion

The small scaled rocket was built for controlling the yaw axis is successfully implemented in this thesis. The root mean square error for distance is 0.6151046 meter and for yaw is 3.7332884 degree. For hardware components, it is quite simple. One body tube and three free wheels are included. At first, the nose cone is intended to add but it only leads to excess load. The heaviness is one of the bad factors for the system to run smoothly. For software implementation, the magnetometer is used to determine which direction that the rocket is pointing, and GPS is used to detect the points that rocket has to go and knowing the distance that has travelled. Butterworth filter is implemented in software section for filtering most of the noise created by magnetometer. The nozzle thrust force pushes and rocket body to turn the free wheels to move to the heading and the directions.

5.2 Recommendation

The next step for this thesis should be trying to fly this with good combustion chamber and fuels. And controlling 3DOF of motion for the rocket and maintain in the air for more than 45 seconds. Since this system is high non-linearity and unstable, the adaptive control theory should be used. In the section of filtering the heading degree, the yaw errors from the GPS tracking analysis, but if the better magnetometer will be used, the performance will be better than this.

REFERENCES

- Bayan AbuShawar, E. A. (2015). ALICE Chatbot: Trials and Outputs. *Computación y Sistemas*.
- Duan, M.-Z. H.-R. (2011). Adaptive Dynamics Surface Control for Integral Missile Guidance and Autopilot. *International Journal of Automation and Computing*, 8(1), 122-127.
- F. Sandoval-Ibarra, M. C.-C.-E.-L.-B. (2011). Design of 2nd order low-pass active filters by preserving the physical. *REVISTA MEXICANA DE FÍSICA E 57 (1)*, 1–10.
- George P. Sutton, O. B. (2000). *Rocket Propulsion Elements (7th Edition)*. New York: JOHN WILEY & SONS, INC.
- Heath, C. (n.d.). *Water Rocket simulation*. Retrieved from Water Rocket simulation: <http://polyplex.org/rockets/simulation/>
- Jing, C. L. (2006). Application of PID Controller to 2D Differential Geometric Guidance and Control Problem. *25th Chinese Control Conference*, 1953-1958.
- Jyothi, V. A. (2020). CFD Analysis of a Solid Propellant Retro Rocket Motor using Ansys Fluent. *E3S Web of Conferences 184:01054*.
- Kunapinun, V. (2011). *BALANCING CONTROL OF A HOVERCRAFT AND TRACKING*. Thailand: Asian Institute of Technology.
- L. Fischer, T. G.-G. (2019). On the approximation of DIY water rocket dynamics including air drag. *Int. J. of Sci. Research in Mathematical and Statistical Sciences*.
- Lacey, T. (n.d.). *Chapter 11 Tutorial: The Kalman Filter*. Retrieved from MIT Open courseware: <http://web.mit.edu/kirtley/kirtley/binlustuff/literature/control/Kalman%20filter.pdf>
- Li, J. Y. (2012). Disturbance Observer Based Model Predictive Control for Autopilot Design of Back-To-Turn Missiles. *Chinese Control and Decision Conference (CCDC)*, 2099-2104.

- Multidimensional Kalman Filter*. (n.d.). Retrieved from Kalman Filter Tutorial:
<https://www.kalmanfilter.net/kalmanmulti.html>
- Nakka, R. (n.d.). *Richard Nakka's Experimental Rocketry Web Site*. Retrieved from
Richard Nakka's Experimental Rocketry Web Site: <http://www.nakka-rocketry.net/>
- NASA. (n.d.). *NASA*. Retrieved from https://www.grc.nasa.gov/WWW/k-12/TRC/Rockets/history_of_rockets.html.
- S. E. Talole, A. A. (2011). Robust Roll Autopilot Design for Tactical Missiles.
Journal of Guidance, Control and Dynamics, 107-116.
- S. N. Balakrishnan, A. T. (2013). *Advances in Missile Guidance, Control and Estimation*. CRC Press: Taylor & Francis Group.
- Siouris, G. M. (2004). *Missile Guidance and Control System*. New York: Springer Press, Springer-Verlag New York, Inc.
- Swarup, S. M. (2017). Robust PID Autopilot Design for Back-To-Turn Missile.
International Conference on Intelligent Computing and Control (I2C2), 1-6.
- Wallace, D. R. (2003). *The Elements of AIML style*.
- Wikipedia. (n.d.). *Haversine formula*. Retrieved from Wikipedia:
https://en.wikipedia.org/wiki/Haversine_formula#:~:text=The%20haversine%20formula%20determines%20the,and%20angles%20of%20spherical%20triangles.